RECURSIVE FILTERS USING CCD'S

by

S. T. Ferguson

A thesis submitted to the School of Graduate Studies in partial fulfillment of the requirements for the degree of Master of Applied Science

Department of Electrical Engineering

University of Ottawa

Ottawa, Canada

June 1977

ABSTRACT

The design and implementation of recursive charge coupled device filters is presented. The characteristics of charge coupled devices are discussed as they apply to such filters. Second order sections are analyzed in terms of coefficient sensitivity. Scaling and pole zero pairing for higher order filters are discussed. The hardware implementations of a second order resonator, a general second order section, and a fifth order low pass filter are presented.

ACKNOWLEDGEMENTS

The author wishes to thank his supervisor, Dr. W. Steenaart, for his guidance, encouragement, and advice throughout the course of this work.

The author is grateful to Dr. A. Ibrahim, T. Foxall, G. Hupé and T. Sellars of the Silicon Technology Laboratory of Bell Northern Research Ltd. for their supplying of devices used in this work, and for their suggestions and advice while the work was in progress.

TABLE OF CONTENTS

LIST OF FIGURES

INTRODUCTION

The few years since 1970 have seen a rapid growth in the application of charge coupled devices to analog and digital signal processing. First reported in 1970[1], these devices now promise to replace passive and active filters in many roles, perform convolutions and spectral analysis, do visible-light and infrared imaging, replace magnetic data recording in some bulk memory systems, and realize very low power logic circuits.

Charge coupled devices(CCD's) consist basically of a series of closely spaced electrodes separated from a monolithic semiconductor substrate by a thin insulating layer, normally silicon dioxide for silicon devices. Charge is introduced at one end of the electrode array, and is manipulated in the substrate by applying voltages to the electrodes in a sequential fashion. The operation of a silicon two phase CCD delay line is illustrated in Figure 1.1. Minority carrier charge is stored at the silicon-silicon dioxide interface because of the potential wells created by the clocking pulses. The quantity of charge normally represents, in some fashion, the input signal voltage sampled at regular intervals at the device input. By nondestructively sensing the charge stored under the appropriate set of electrodes, time delayed versions of the input signal are obtained at delays of T, 2T, ... nT seconds, where 1/T is the rate of input sampling.

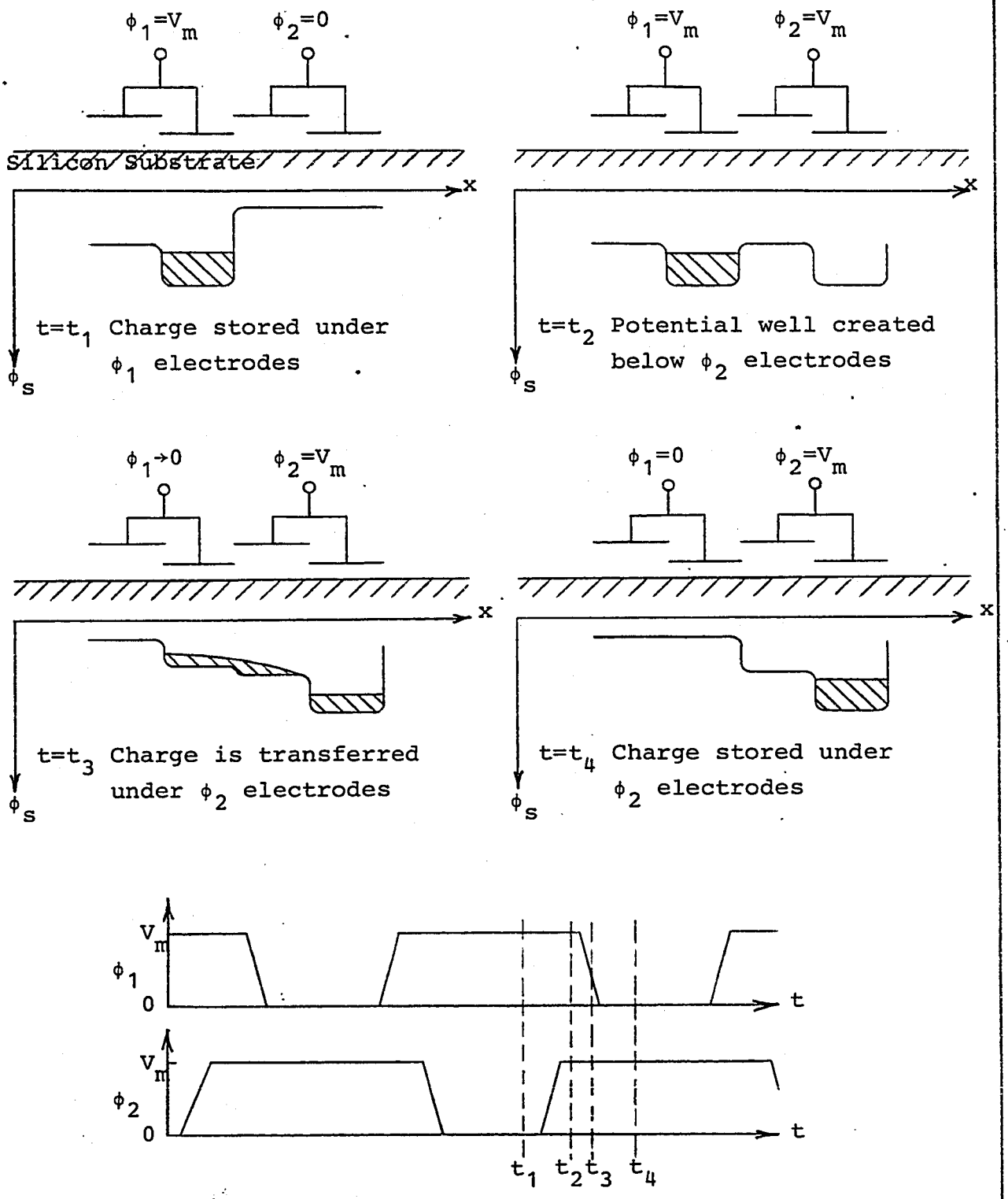

Figure 1.1 Two Phase CCD Operation

In sampled data filtering, transfer functions are realized of the form

$$H(Z)=\frac{\sum_{k=0}^{M} a_k Z^{-k}}{1+\sum_{\ell=1}^{N} b_\ell Z^{-\ell}} \qquad (1.1)$$

where H(Z) is the Z-transform of the discrete impulse response of the filter; a_k and b_ℓ are coefficients set by the particular design of the filter; and Z^{-1} is the unit delay operator, representing a delay of T seconds. One structure capable of realizing H(Z) is shown in Figure 1.2. The coefficients a_k are known as the feedforward terms, while the coefficients b_ℓ are known as the feedback terms. Filters in which all $b_\ell=0$ are called transversal filters. Much work has been done to realize such filters both in digital and in analog sampled data form. Filters in which $b_\ell \neq 0$, for $\ell<N$, are known as recursive filters, where N is the order of the filter. Recursive filters have been built using digital and sampled data analog techniques[2,3,4,5].

A technique which is now used in almost all CCD transversal filters, and which enables most of the filtering operations to be accomplished directly in the CCD structure itself, is the split-electrode sensing technique [6]. A typical split-electrode structure is shown in figure 1.3. Each side of every split electrode is connected to a common bus,

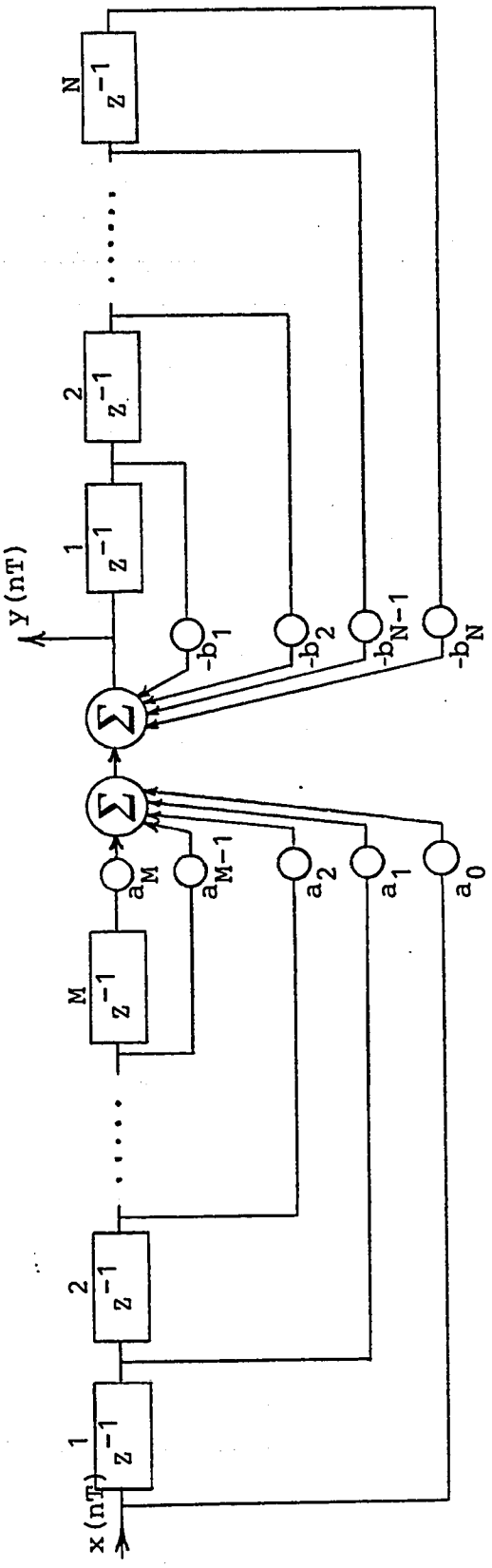

Figure 1.2 Structure to Realize H(Z)

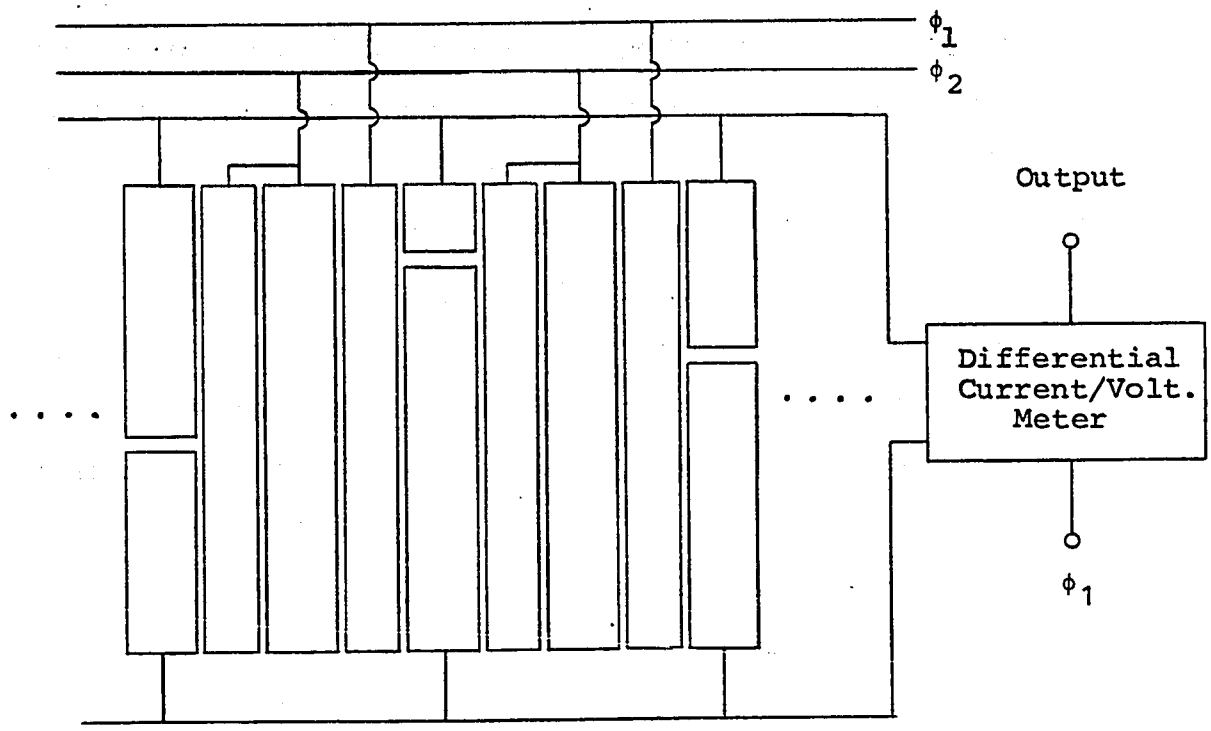

Figure 1.3 Split Electrode Structure

and the voltage or current changes in the busses are differentially combined to produce a weighted sum of delayed signal samples. This operation performs the filtering function. In this manner, coefficients or "tap weights" within the range -1 to +1 can be realized. In recursive filters a weighted sum of delayed signal samples is added to the input signal. Coefficients b_1 in the range -2 to +2 for second order filters are possible, and larger coefficients may be required for higher order filters. This requirement makes the realization of CCD recursive filters more complex than that of transversal filters.

This thesis reports on an analysis of recursive sampled data filters, and presents the realization of three recursive CCD filters. In Chapter 2, the two level, polysilicon gate CCD used to construct the filters is discussed, and the non-ideal effects of the CCD are reviewed. In Chapter 3 the theory of recursive filtering is discussed, including considerations of sensitivity and stability. An analysis of the second order recursive filter, which can be used as a building block to construct higher order filters, is presented in Chapter 4. In Chapters 5, 6 and 7, measured data are compared with computed values for a second order resonator, a general second order section, and a fifth order filter of cascade structure, respectively. Several applications for recursive CCD filters are described in Chapter 8.

CHARGE COUPLED DEVICE CHARACTERISTICS

2.1 Input and Output Methods

The CCD used in all of the experimental work reported here, is a Bell Northern Research two level polysilicon gate device designated CCRF01. As an element in the realization of sampled data recursive filters, the primary interest is in the CCD properties of sampling and delaying a signal in discrete time steps, and in weighting delayed samples with preset multipliers. Ideally, there are no nonlinearities present in the transfer function which relates the voltage output at any tap on the CCD to the input voltage representing the signal. In practice, however, nonlinearities do result from the voltage to charge conversion at the input and the charge to voltage conversion at any of the sensing electrodes.

The two methods of charge input employed in the CCRF01 device are shown in Figure 2.1. The gate input method, Figure 2.1a, produces a charge input to the CCD proportional to the input signal applied on gate G_2. Gate G_1 is driven with the sampling pulse, forming a channel through which charge flows from the grounded source electrode S to equalize the surface potential under G_2 with that at S. Thus a "bucket", whose depth is proportional to the input signal, is "filled" with charge. This charge is then transferred along the CCD by the ϕ_1 and ϕ_2 electrodes. Nonlinearities arise from a portion of

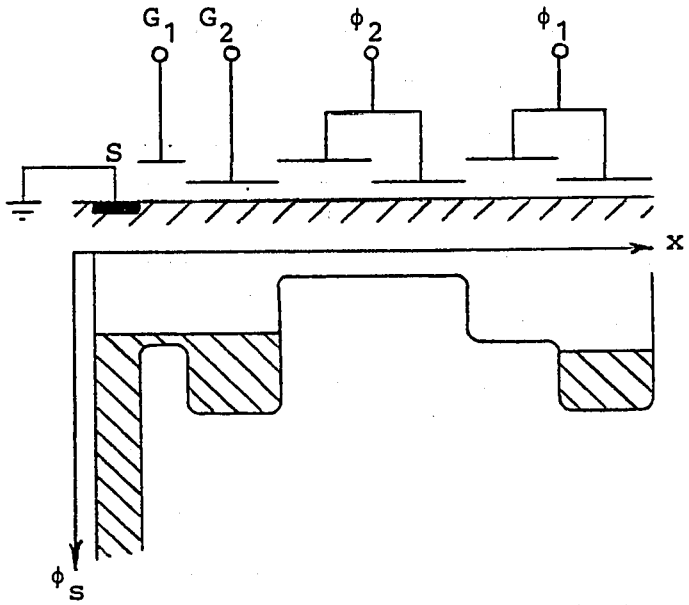

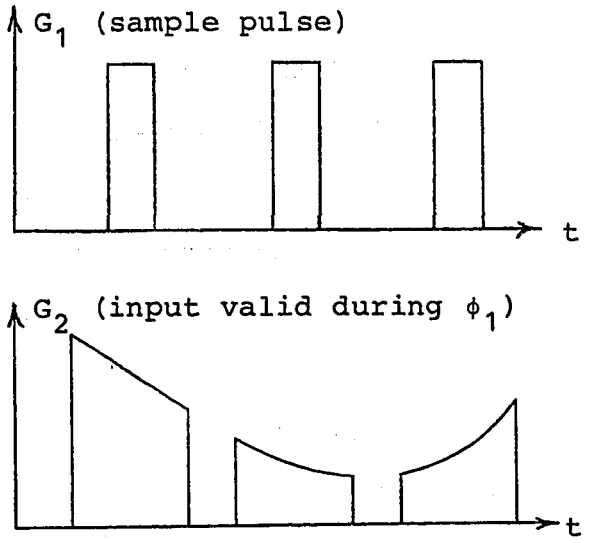

Figure 2.1a Gate Input Method

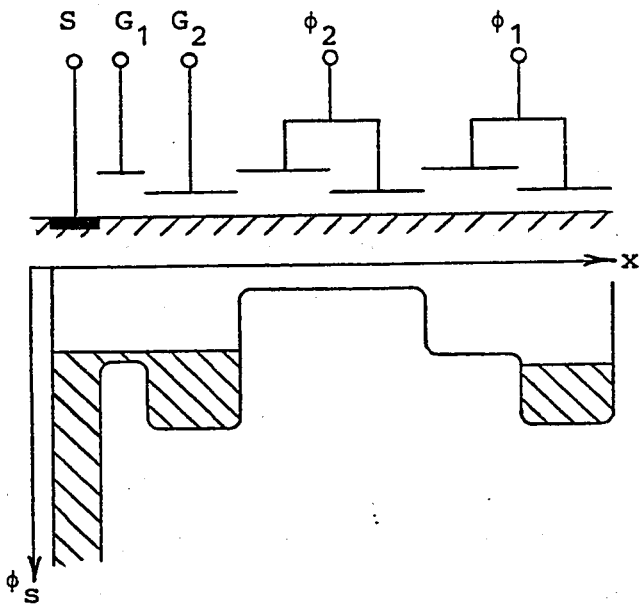

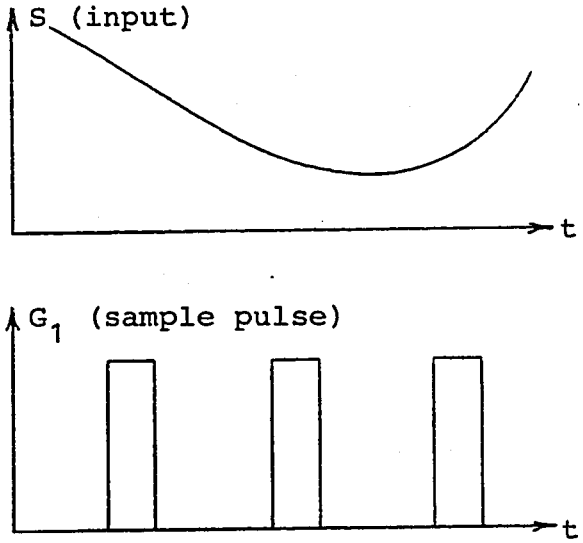

Figure 2.1b Source Input Method

Figure 2.1 CCD Charge Input Methods

the charge under G_1 spilling over to G_2 when the sampling pulse goes to its low level. This can be reduced by making the active area under G_1 as small as possible.

The input method of Figure 2.1b, here referred to as the source input method[8], produces a charge inversely proportional to the input signal applied to the source S. Gate G_1 is again driven by the sampling pulse, while gate G_2 is held at a reference potential during the ϕ_1 clock interval, forming an input bucket. The surface potential under G_2 is equalized with the input voltage on S when G_1 is pulsed to a high level filling the bucket with an amount of charge proportional to the difference between the reference potential well and the input voltage. The charge is then transferred along the CCD in the same manner as before. A nonlinearity is introduced by the dependence of the substrate to G_2 capacitance on the surface potential under G_2, and on the input signal. Another nonlinear effect is introduced by the spilling of charge under G_1 into the G_2 bucket, as in the gate input method.

The CCD output method used in this work is the floating gate sensing method[9] illustrated in Figure 2.2. An output voltage is obtained by nondestructively sensing the amount of charge under the ϕ_1 electrode. A ϕ_3 clock pulse presets the sensing electrode G to a potential V_{dd} prior to charge transfer from the ϕ_2 electrode, then G is allowed to float. When the charge is pushed to G by the ϕ_2 electrode falling to

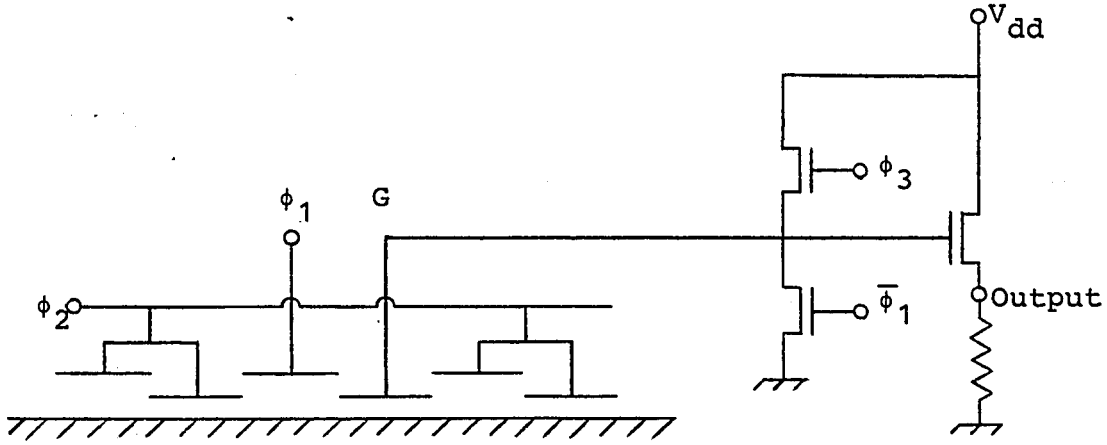

Figure 2.2a Sensing Circuit

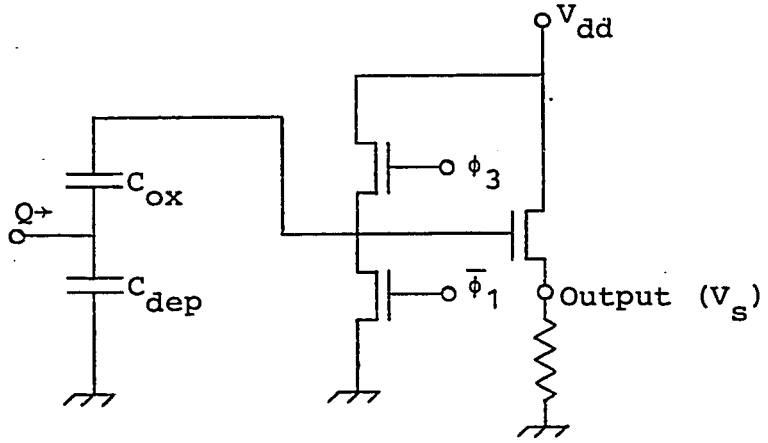

Figure 2.2b Equivalent Circuit

Figure 2.2 CCD Floating Gate Sensing Method

a low potential, G drops to a lower potential from its floating value of V_{dd}. This potential change is buffered by an on-chip source follower, and an output signal is obtained across an external resistor to ground. The sensed voltage change is a non-linear function of the charge transferred, as a study of Figure 2.2b will show. A charge Q added to the junction of the oxide capacitance(C_{ox}) and the depletion capacitance(C_{dep}) will cause no charge redistribution on C_{ox} because the upper plate charge is fixed due to its being floated. Q, however, will cause the potential across C_{dep} to drop thus causing a similar voltage drop in V_s. C_{dep} is a nonlinear capacitor and thus V_s will not change by a linear function of Q. Operating the CCD with a bias charge or "fat zero" and having the signal variations cause a sufficiently small change in the bias charge, reduces the sensing distortion to an acceptable level.

2.2 Non Ideal CCD Effects

2.2.1 Charge Transfer Efficiency

Charge transfer efficiency of CCD's[10] expresses the fractional amount of charge transferred from one potential well to the next in response to the clocking pulses. This

phenomenon causes a small amount of charge to be added to the adjacent charge packet. The figure ε is normally used to express the ratio:

$$\varepsilon = \frac{\text{untransferred charge on k'th stage}}{\text{charge initially on k'th stage}} \qquad (2.1)$$

and $\rho = 1-\varepsilon$

where ρ is the charge transfer efficiency, which for practical devices can be as high as .9999. For a simple delay line the effect of charge transfer efficiency will manifest itself as a transfer function at the k'th output stage of[11]

$$\frac{V_k(Z)}{V(Z)} = \left[\frac{1-\varepsilon}{1-\varepsilon Z^{-1}}\right]^k Z^{-k} \qquad (2.2)$$

where $V(Z)$ and $V_k(Z)$ are the Z-transforms of the input voltage to the CCD and the output voltage at the k'th stage, respectively. It should be noted that ε refers to the charge lost in the transfer from one output stage to the next; that is, two transfers for a two-phase CCD. For a single delay stage this reduces to

$$\frac{V_{i+1}(Z)}{V_i(Z)} = \frac{\rho Z^{-1}}{1-\varepsilon Z^{-1}} \equiv P(Z^{-1}) \qquad (2.3)$$

The effect on any filter transfer function realized using the CCD can thus be found by substituting $P(Z^{-1})$ for Z^{-1}.

2.2.2 Gain and Gain Stability

The gain of the i'th stage of a CCD delay line can be defined as the ratio of the output voltage at the i'th sensing electrode to the input voltage to the CCD. When using external multipliers to realize tap weights for a filter, the value of any tap weight will change proportionally to the gain of the appropriate stage. For a transversal filter the transfer function is:

$$H(Z)=\sum_{k=0}^{N} a_k Z^{-k} \tag{2.4}$$

A common factor can be removed from each of the tap weights a_k leaving

$$H(Z)=A\sum_{k=0}^{N} a'_k Z^{-k} \tag{2.5}$$

where $Aa'_k = a_k$. Assuming that the coefficients a_k are realized exactly, the value of A can represent the gain of the CCD, which can vary with the operating parameters. Variations in A will cause a magnitude change in the filter transfer function but will not move the zeros of the filter, and thus not change the shape of the frequency response. For a recursive filter with transfer function

$$H(Z)=\frac{\sum_{k=0}^{M} a_k Z^{-k}}{1+\sum_{\ell=1}^{N} b_\ell Z^{-\ell}} \tag{2.6}$$

a common factor may be removed from the numerator without a shift of the filter zeros, but not from the denominator without changing the pole locations, since the "1" is a function of the filter structure and cannot be changed. A change in the CCD gain causes a new transfer function to be realized as

$$H'(Z)=\frac{\sum_{k=0}^{M} a'_k z^{-k}}{1+\sum_{\ell=1}^{N} b'_\ell z^{-\ell}} \qquad (2.7)$$

so that the filter poles (roots of the denominator) have been moved from their designed locations. The CCD gain variations must then be considered in the total allowable coefficient error when the filter is being designed.

The gain of the CCD used in this work was measured by applying an AC signal to the gate and the source inputs in turn, and measuring the output at tap number one for values of the drain voltage (V_{DD}) from 10 to 16 V and substrate bias between 1 and 7 V. Harmonic distortion at the output was similarly measured. The measured values of gain and harmonic distortion are plotted in Figures 2.3 and 2.4 for the gate and source inputs respectively. From these plots a suitable operating range for the CCD can be chosen, as indicated by the area marked in the figures, where harmonic distortion is better than 40 dB and gain variations are held to within $\pm$1%.

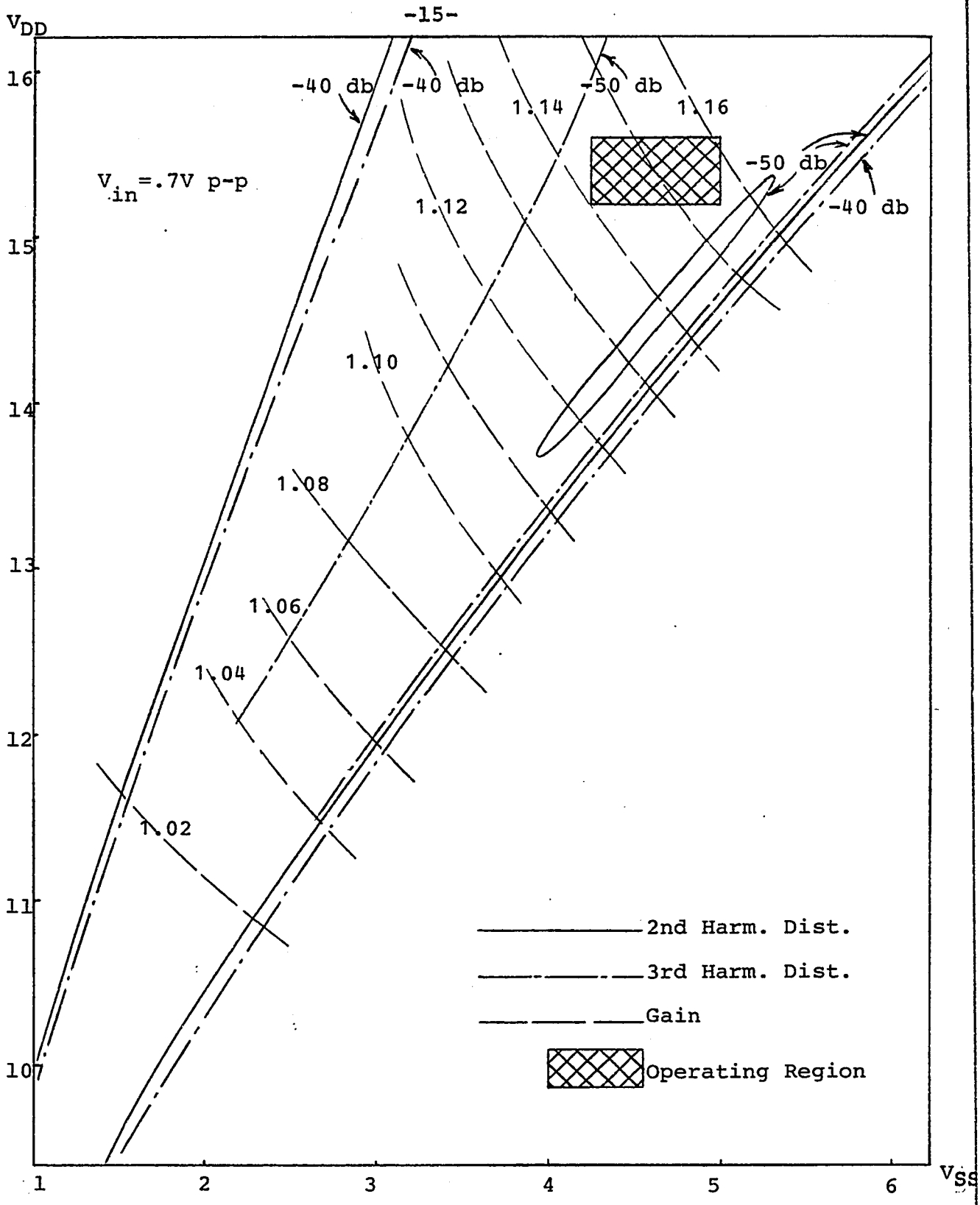

Figure 2.3 Gain and Harmonic Distortion Source Input Method

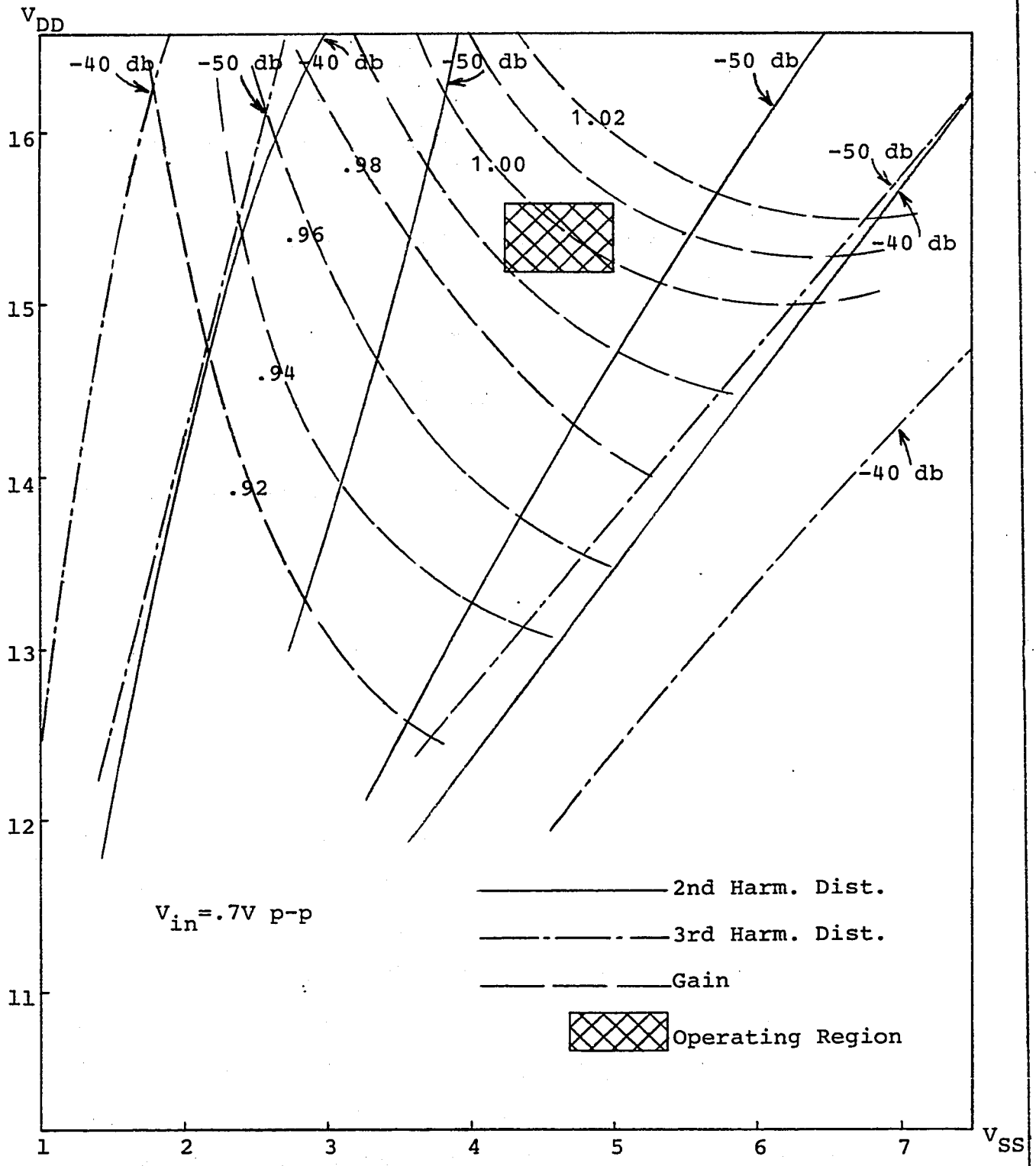

Figure 2.4 Gain and Harmonic Distortion Gate Input Method

RECURSIVE FILTERS

3.1 Infinite Impulse Response Structures

A network transfer function of the form

$$H(Z)=\frac{\sum_{k=0}^{M} a_k z^{-k}}{1+\sum_{\ell=1}^{N} b_\ell z^{-\ell}} \tag{3.1}$$

realizes a system with a difference equation

$$y(nT)=\sum_{\ell=1}^{N} b_\ell y(nT-\ell T)+\sum_{k=0}^{M} a_k x(nT-kT) \tag{3.2}$$

By inspection, the network corresponding to this difference equation can be drawn as in Figure 3.1a and is known as the direct form I realization[12]. Since this realization is in fact the cascade of two networks, one realizing the zeroes of the transfer function H(Z) and the other the poles, the order can be reversed to give the network of Figure 3.1b. It is now observed that the two delay branches have the same input and thus can be replaced with only one delay branch, as shown in Figure 3.1c. This structure is known as the direct form II[13], and is also one of the canonic forms since it contains the minimum number of delays necessary to realize H(Z). Any of the coefficients a_k or b_ℓ can be zero in these structures. For real a_k and b_ℓ, H(Z) can be factored into quadratic factors in

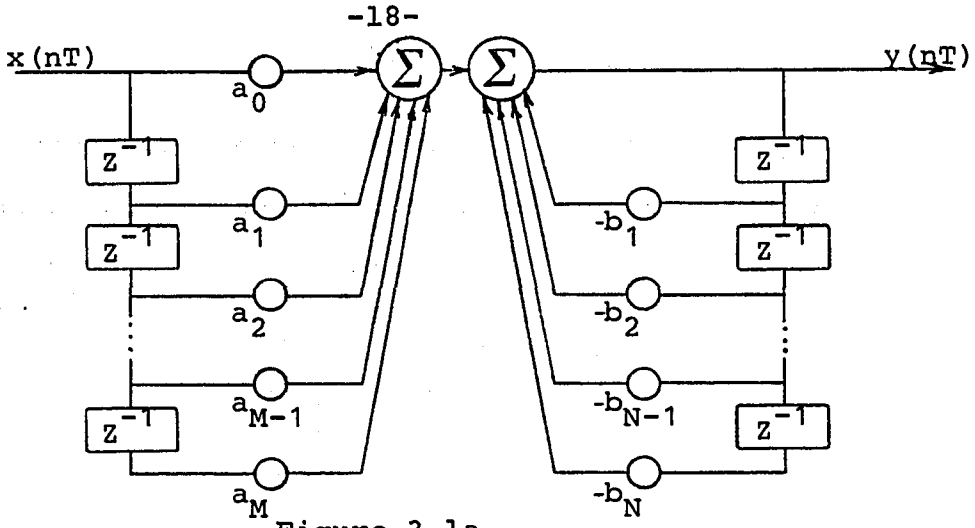

Figure 3.1a

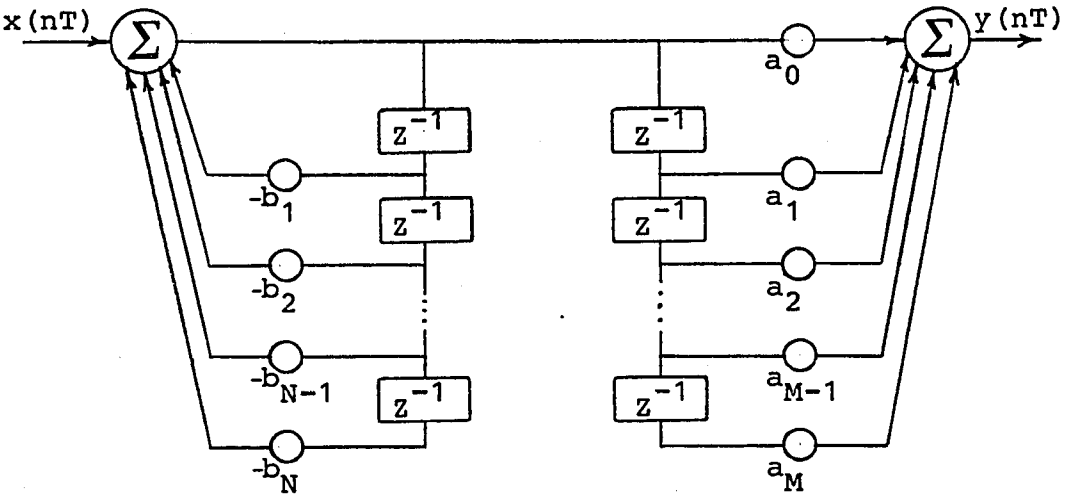

Figure 3.1b

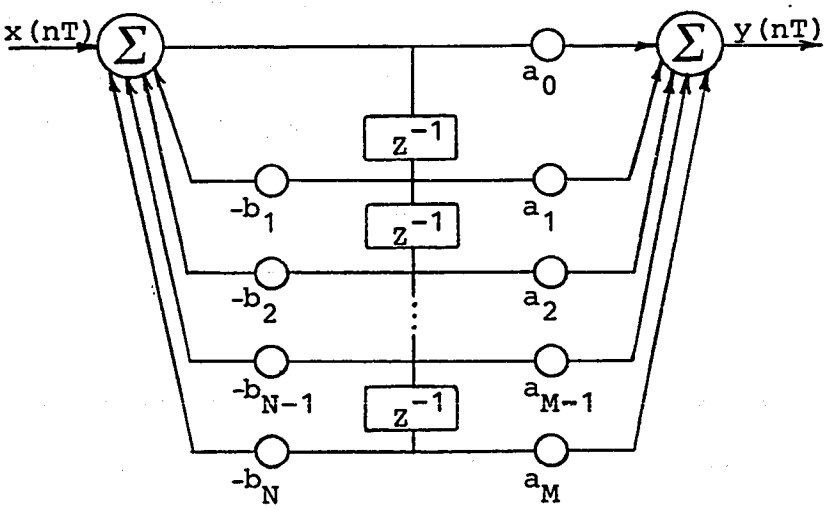

Figure 3.1c

Figure 3.1 Infinitive Impulse Response Networks

the numerator and denominator if M and N are even, or quadratic factors and a first order factor if M and/or N are odd. Thus, for M and N even,

$$H(Z)=A\frac{\prod_{k=1}^{M/2}(1+\alpha_{1k}Z^{-1}+\alpha_{2k}Z^{-2})}{\prod_{k=1}^{N/2}(1+\beta_{1k}Z^{-1}+\beta_{2k}Z^{-2})} \tag{3.3}$$

and for M and N odd,

$$H(Z)=A\frac{(1+\alpha_0Z^{-1})\prod_{k=1}^{\frac{M-1}{2}}(1+\alpha_{1k}Z^{-1}+\alpha_{2k}Z^{-2})}{(1+\beta_0Z^{-1})\prod_{k=1}^{\frac{N-1}{2}}(1+\beta_{1k}Z^{-1}+\beta_{2k}Z^{-2})} \tag{3.4}$$

These representations suggest a cascade structure of first and second order sections with factors from the numerator and denominator arbitrarily paired. Each section can be realized in the direct form II, as shown in Figure 3.2.

A partial fraction expansion of H(Z) into a sum of quadratic factors of the form

$$H(Z)=\sum_{k=1}^{N/2}\frac{\gamma_{0k}+\gamma_{1k}Z^{-1}}{1+\beta_{1k}Z^{-1}+\beta_{2k}Z^{-2}} \quad \text{(here M=N, even)} \tag{3.5}$$

allows a parallel realization of the filter, as shown in Figure 3.3. Realization of a filter with second order sections

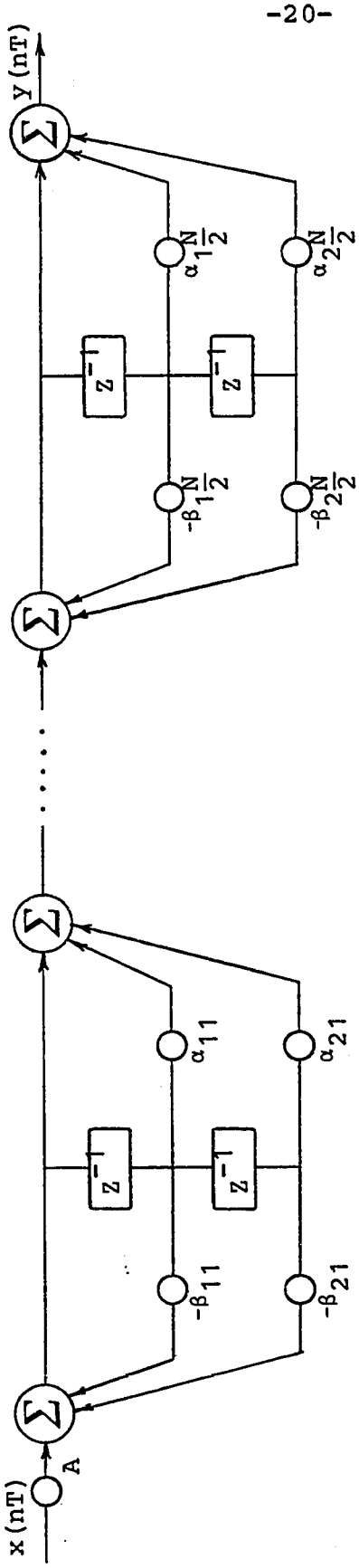

Figure 3.2 Cascade Filter Realization (M=N, even)

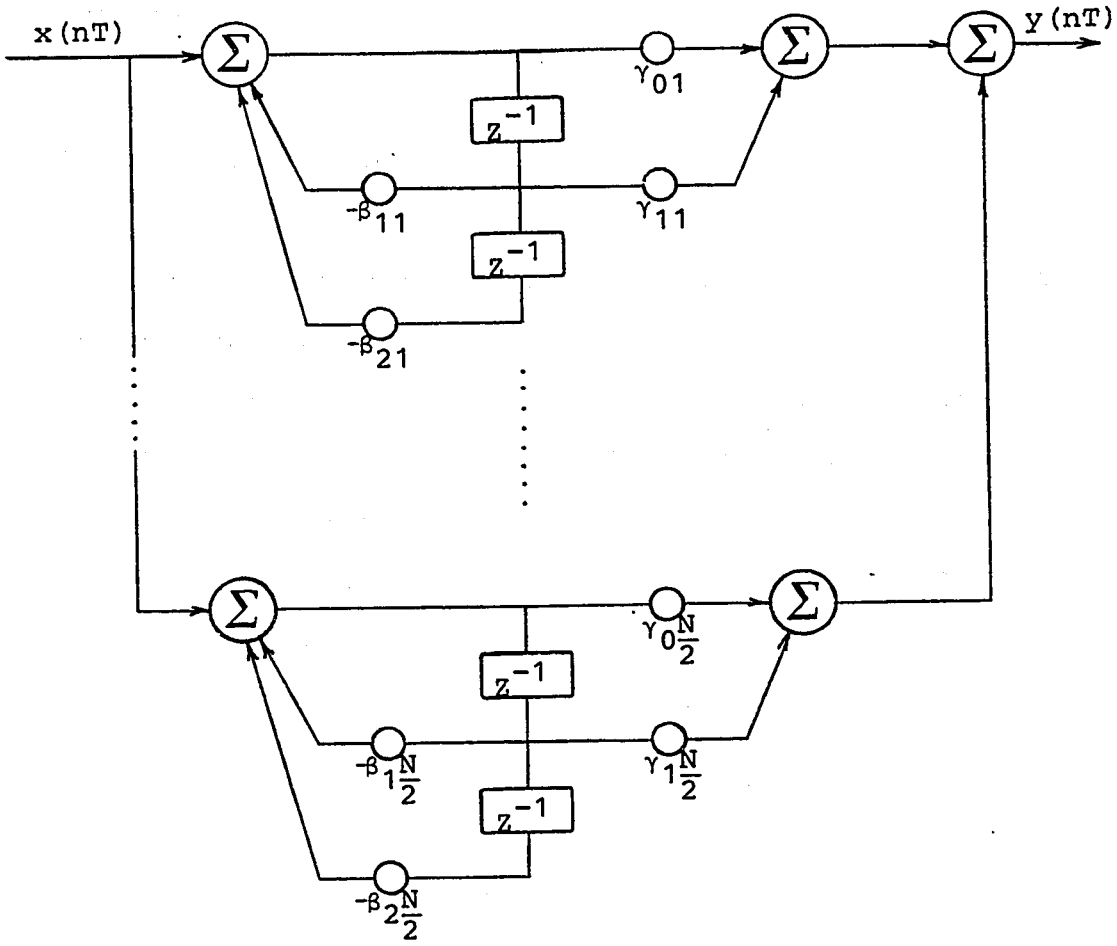

Figure 3.3 Parallel Filter Realization (M=N, even)

offers benefits in terms of the accuracy with which coefficients must be realized to maintain acceptable performance.

3.2 Coefficient Sensitivity

In the hardware realization of sampled data filters, it is of great concern whether or not the filter response will meet the design requirements with a given accuracy to which the filter coefficients a_k and b_ℓ can be realized. As an example, a design for an elliptic function low pass filter may have a pass-band ripple of .1 dB, yet when realized with coefficients accurate to ±.5% the ripple increases to 1 dB, a value which would probably be unacceptable. A direct form filter designed with a transfer function

$$H(Z)=\frac{\sum_{k=0}^{M} a_k Z^{-k}}{1+\sum_{\ell=1}^{N} b_\ell Z^{-\ell}} \tag{3.5}$$

when realized with inaccurate coefficients $a'_k=a_k+\Delta a_k$ and $b'_\ell=b_\ell+\Delta b_\ell$ now has a transfer function

$$H'(Z)=\frac{\sum_{k=0}^{M} a'_k Z^{-k}}{1+\sum_{\ell=1}^{N} b'_\ell Z^{-\ell}} \tag{3.6}$$

If H(Z) has poles located at $Z=Z_i$ $i=1,2,\ldots,N$ then H'(Z) will have poles located at $Z=Z_i+\Delta Z_i$; that is, they will have migrated from their intended locations due to the inaccuracies Δb_ℓ. Similarly, the zeroes will migrate to new locations. Kaiser[14] and Oppenheim and Schafer[15] have shown that the sensitivity of a simple order complex pole, Z_i, to a change in the coefficient b_ℓ, can be expressed by

$$\frac{\delta Z_i}{\delta b_\ell} = \frac{Z_i^{N-1}}{\prod_{\substack{k=1 \\ k\neq\ell}}^{N} (Z_i - Z_k)} \tag{3.7}$$

Mitra and Sherwood[16] have expressed the change in the radius and the angle of a pole as

$$\Delta r_i = S_b^{r_i} . \Delta B \tag{3.8}$$

$$\Delta \theta_i = S_b^{\theta_i} . \Delta B \tag{3.9}$$

where $S_b^{r_i}$ and $S_b^{\theta_i}$ are row vectors incorporating the initial pole locations, and ΔB is a column vector of the coefficient changes Δb_ℓ. A Fortran program was written to evaluate pole changes for several fourth order filters. In particular, the case of a filter with two pairs of closely spaced poles was studied. Coefficient errors were assumed to be of the form

$$\Delta b_\ell = x.E.[b_i] \tag{3.10}$$

x=uniformly distributed random variable
E=maximum coefficient error
$[b_i]=\max\{b_1, b_2, \ldots, b_N\}$

For the case of poles separated slightly in radius, as in Figure 3.4a, reducing the difference in radius caused large pole migrations in the radial direction, whereas poles of the same radius but separated in angle (Figure 3.4b) were caused to change in angle by large amounts. Figure 3.4c shows the rapid increase in pole angle error for the case where the poles were of the same radius and the angle between them was decreased. From a few computer simulations it became evident that second order filters were the most complex that could be realized with coefficient accuracy on the order of 0.1%, and that higher order filters would of necessity be composed of second order sections. This result has been presented previously in the literature[17].

Should the coefficient inaccuracies be such as to move the poles of the filter outside the unit circle, the filter will become unstable[18]. Thus a rough bound on necessary coefficient accuracy can be found from the criterion for stability; that is, all poles lie inside the unit circle. Such a bound is used in Chapter four for the second order case.

3.3 Pole-Zero Locations of Filter Functions

Some general comments can be made about the pole and zero locations of sampled data filter functions to show the role of poles and zeroes in shaping the frequency response. The

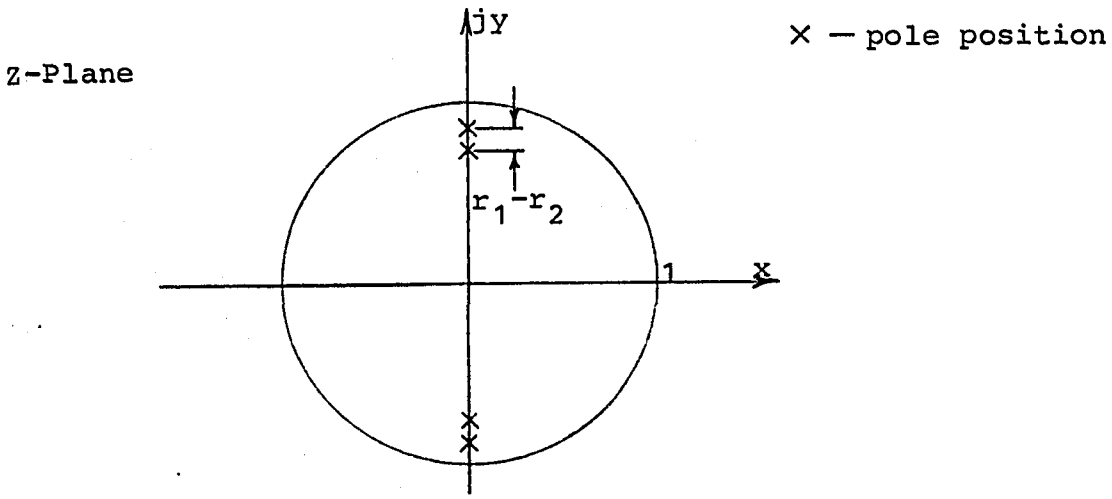

Figure 3.4a

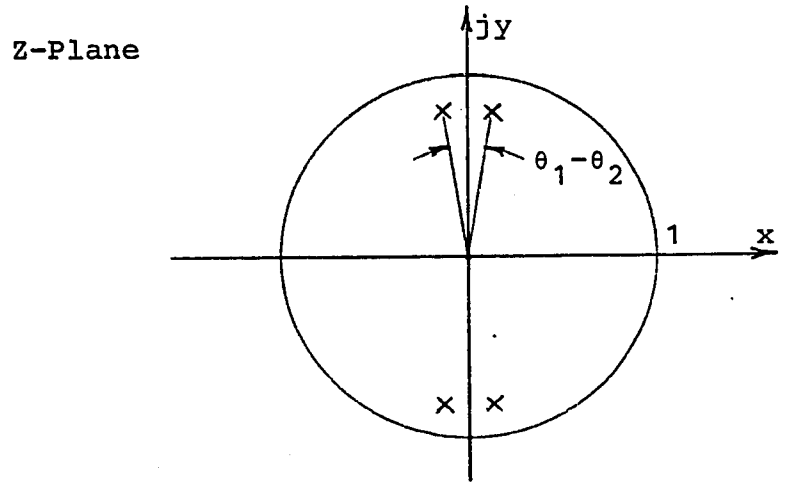

Figure 3.4b

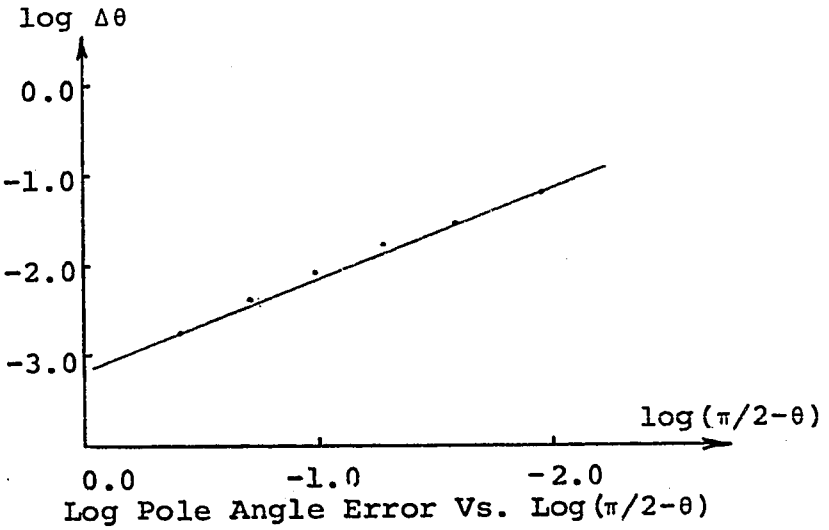

Log Pole Angle Error Vs. Log(π/2-θ)

Figure 3.4c

Figure 3.4 Effect of Coefficient Error for Fourth Order Resonators

frequency response of a filter can be found by evaluating the transfer function H(Z) on the unit circle in the Z plane, that is by evaluating $H(e^{j\omega T})$. By examining the transfer function in a factored form,

$$H(Z)=A\frac{\prod_{k=1}^{M}\frac{1}{Z_k}-Z^{-1}}{\prod_{\ell=1}^{N}\frac{1}{P_\ell}-Z^{-1}} \qquad \begin{matrix} Z_k=\text{zeroes of } H(Z) \\ P_\ell=\text{poles of } H(Z) \end{matrix} \tag{3.11}$$

$$=A\frac{Z^N P_1 P_2 \ldots P_N \prod_{k=1}^{M}(Z-Z_k)}{Z^M Z_1 Z_2 \ldots Z_M \prod_{\ell=1}^{N}(Z-P_\ell)} \tag{3.12}$$

$$=A\ Z^{N-M}\ Re^{j\Theta}\frac{\prod_{k=1}^{M}(Z-Z_k)}{\prod_{\ell=1}^{N}(Z-P_\ell)} \tag{3.13}$$

and substituting $Z=e^{j\omega T}$,

$$H(e^{j\omega T})=A\ e^{j(N-M)\omega T}\ Re^{j\Theta}\frac{\prod_{k=1}^{M}(e^{j\omega T}-r_k^z e^{j\theta_k^z})}{\prod_{\ell=1}^{N}(e^{j\omega T}-r_\ell^p e^{j\theta_\ell^p})} \tag{3.14}$$

it is observed that the factors each represent a vector from the point on the unit circle for a frequency ω to the zero or pole. This is illustrated in Figure 3.5. For a pole close to the unit circle, as P_1 in Figure 3.5, it can be seen that the vector from that pole is very small when the unit circle is traversed close to the pole, making the denominator of 3.14

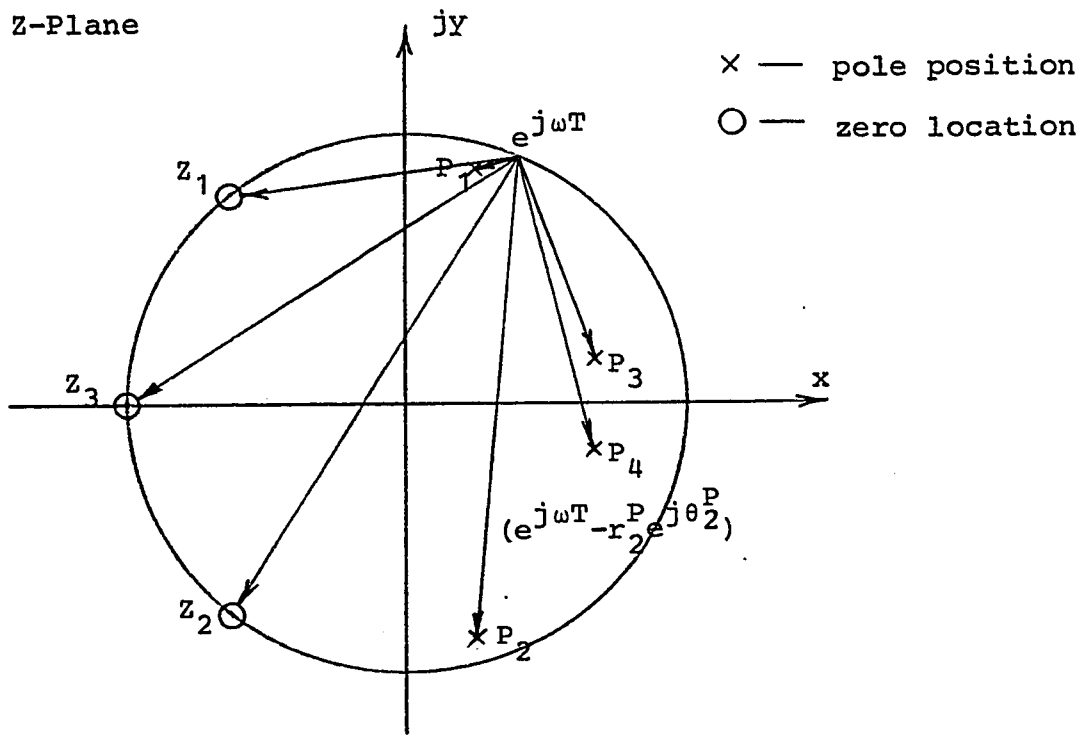

Figure 3.5 Vectors Contributing to Frequency Response

small and consequently $H(e^{j\omega T})$ large. For zeroes on the unit circle, the vector is of zero length when ωT equals the angle of a zero, and thus $H(e^{j\omega T})$ is zero. The frequency response of a filter is made up of the contributions of several poles and zeroes, causing peaks when ωT is close to a pole angle, and nulls when ωT is at the angle of a zero of radius 1. For a typical low pass filter, the pole and zero "constellation" is shown in Figure 3.6.

3.4 The Bilinear Transformation

A method for designing sampled data filters is to use the bilinear transformation to find H(Z) from a continuous time prototype function H(S) [19]. This transformation is very useful if the frequency domain magnitude characteristics are to be preserved in the transformation. Sampled data elliptic function filters, with equiripple passband and stopband performance and the sharpest transition for a given order, can be designed with the bilinear transformation. The mapping from S plane to Z plane is:

$$S \rightarrow \frac{2}{T}\,\frac{Z-1}{Z+1} \qquad (3.15)$$

where the choice of T determines the location of the band edges on the Z plane unit circle. A method of scaling the transformation is to observe that the point on the real

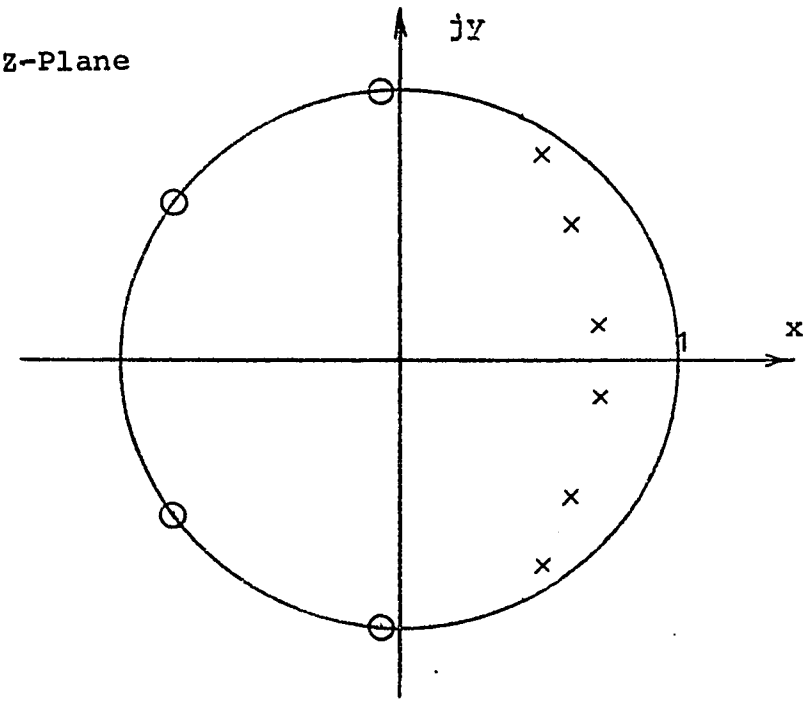

Figure 3.6 Low Pass Filter Pole-Zero Constellation

frequency axis in the S plane representing the band edge of a low pass or high pass filter ($\omega=\omega_p=1$ for normalized filters) maps into the point on the unit circle in the Z plane which represents the band edge ($Z=e^{j\Omega_p T}$). This is illustrated in Figure 3.7. Using the "frequency warping" relationship[20] which can be obtained from 3.15,

$$\omega=\frac{2}{T}\tan\frac{\Omega T}{2} \qquad \begin{matrix}\omega=\text{S plane real freq. variable}\\ \Omega=\text{Z plane real freq. variable}\end{matrix} \qquad (3.16)$$

the desired value of $\Omega_p T$ and the known value ω_p can be substituted in order to find T. As an example, a normalized S plane low pass filter for which $\omega_p=1$ is to be transformed to a Z plane low pass filter where $\Omega_p T$ is 1/10 of the clock frequency; that is, $\Omega_p T=2\pi/10$.

$$\omega_p=\frac{2}{T}\tan\frac{\Omega_p T}{2}$$

$$1=\frac{2}{T}\tan\tfrac{1}{2}\cdot\frac{2\pi}{10}$$

$$T=.649839$$

This value of T can be substituted into equation 3.15 to effect the transformation. It should be noted that when the filter is constructed it is not necessary to use this value of T to determine the clock rate, a filter has been designed only with a pass band edge equal to 1/10 of the clock frequency. Band pass and band stop filters require prewarping of the band edge frequencies before the S plane filter is designed.

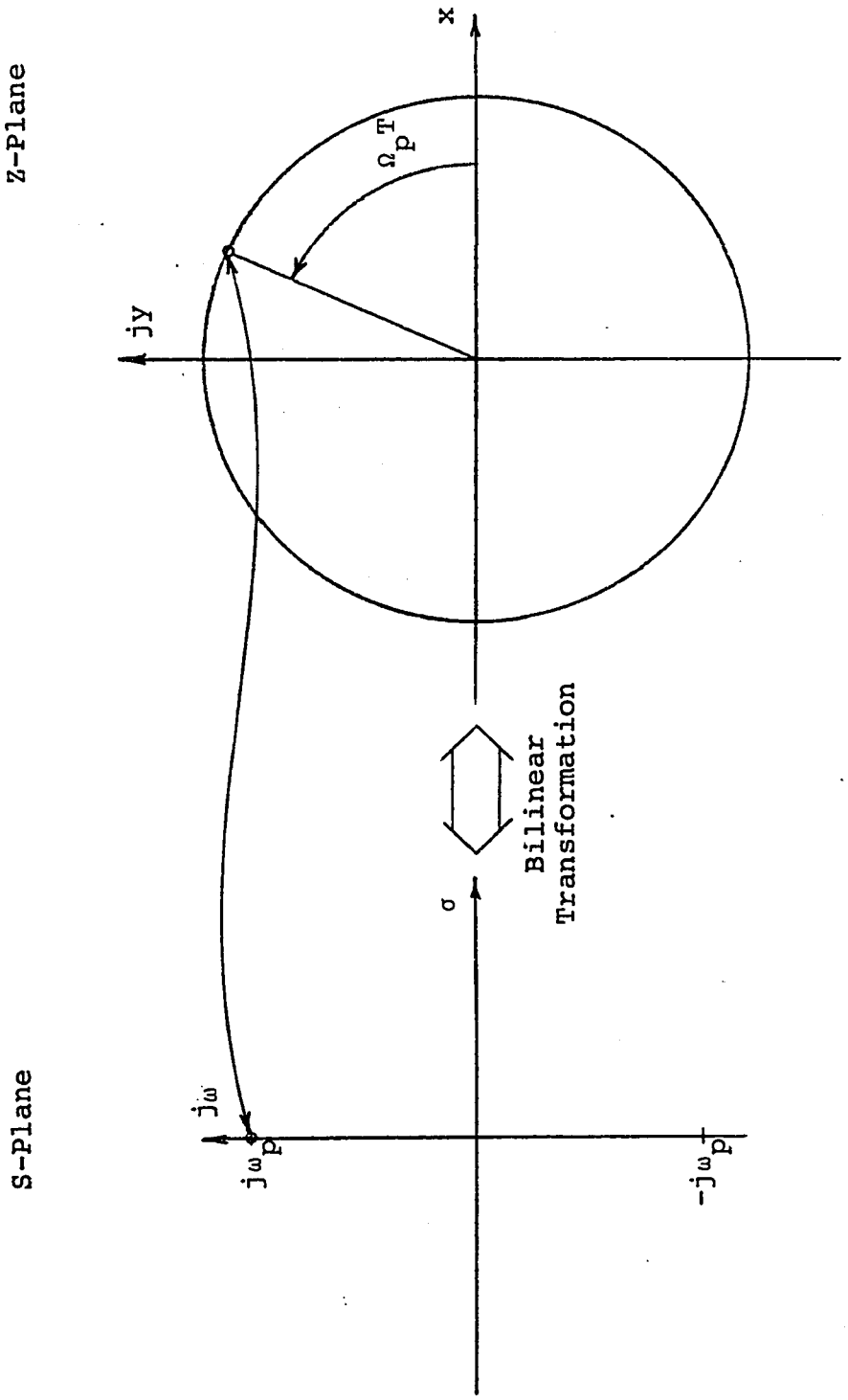

Figure 3.7 Relationship of Band Edge Frequency Through the Bilinear Transformation

SECOND ORDER FILTER SECTIONS

4.1 Filter Structures

Interconnection of second order filter sections ("biquads" in active filter terminology) makes it possible to realize filter functions of any order. Many configurations of the second order section are possible[21,22], however a study of those presented in the literature has led to the conclusion that the direct form II is the most suitable for CCD implementation. This is the case because the delay elements do not have adders between them, leading to efficient CCD realization. Other configurations which have more adders or multipliers than the canonic form lead to increased circuit complexity, with no benefit in terms of reduced coefficient sensitivity. The direct form I would be suitable for CCD implementation, however it has twice as many delay stages as the direct form II, and it does not offer any sensitivity improvement.

A CCD realization of a second order section with no feedback terms (ie a transversal filter) and using the split electrode coefficient weighting technique is illustrated in Figure 4.1a. Transfer electrodes between the sensing electrodes are necessary for charge transfer, but are not shown here for clarity. The input voltage is converted to a charge at the input electrode, and transferred along the CCD

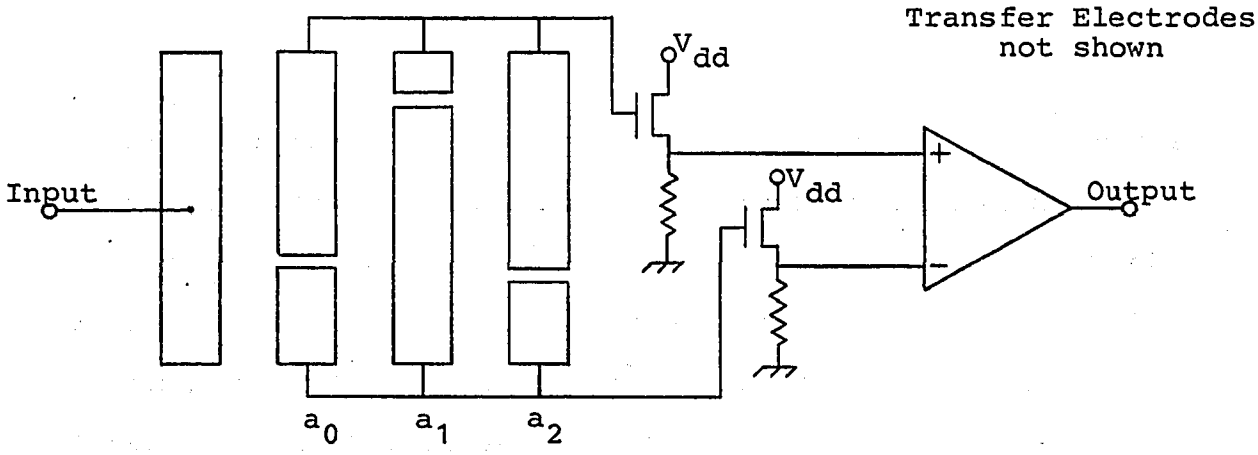

Figure 4.1a

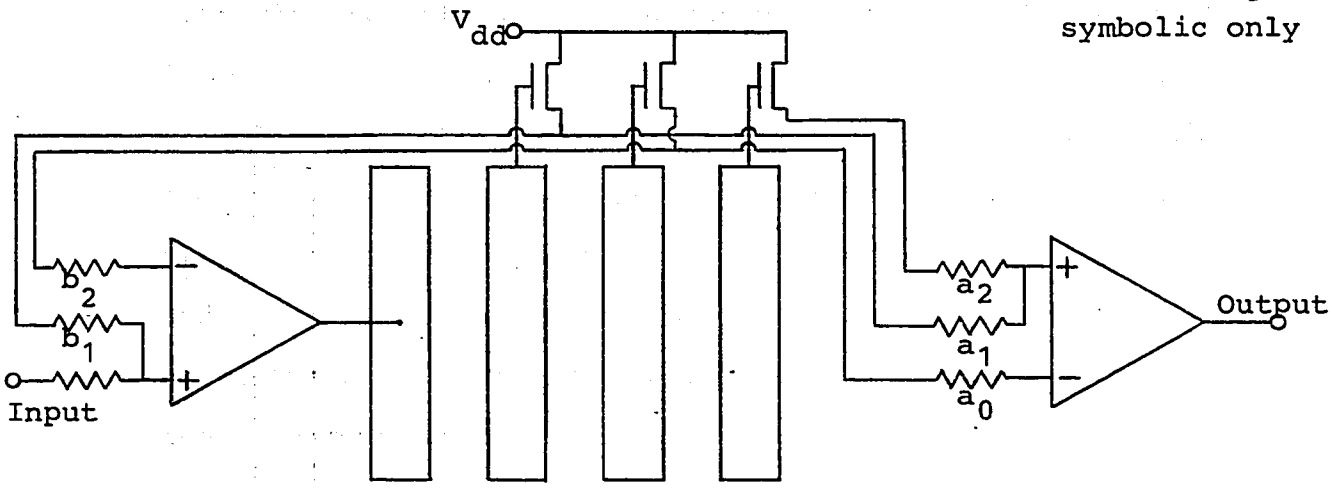

Figure 4.1b

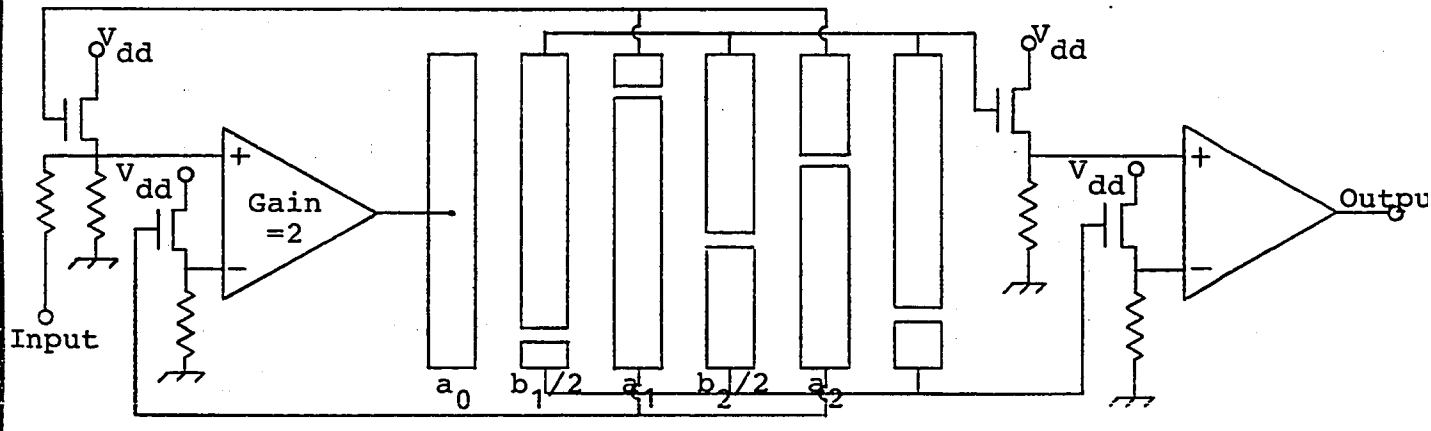

Figure 4.1c

Figure 4.1 CCD Filter Structures

where it is sensed at multiples of the clock period T by the split electrodes. The sensing circuit and operational amplifier perform a sum of the delayed signal samples weighted according to the positions of the splits. Coefficient values ranging from -1 to +1 can be realized in this manner. An extra delay T is added because the first tap, a_0, cannot be taken directly from the input electrode. In most applications this is of no consequence.

A second order section with feedback elements is shown in Figure 4.1b. Here the split electrode technique cannot be used because the first two stages must provide both a feedforward and a feedback term each. The floating gate sensing method is used, with resistors and operational amplifiers providing coefficients. In order to use split electrode weighting to realize both sets of coefficients, the taps can be staggered as in Figure 4.1c. In this case the delay between adjacent feedforward coefficients and adjacent feedback coefficients is two clock periods, causing the frequency response of the filter to become $H(e^{2j\omega T})$, where $H(e^{j\omega T})$ is the response for a single delay T between adjacent feedforward or feedback taps. Using this scheme the CCD filter would have to be operated at twice the clock frequency needed if the scheme of Figure 4.1b were used.

4.2 Second Order Sampled Data Resonator

A second order section realizing a complex conjugate pair of poles is useful as a narrow band pass filter, or "sampled data resonator". Several examples using CCD's and bucket brigade devices (BBD's) in multiplexed and non-multiplexed filters have been reported[2,3,5]. A measure of the frequency selective properties of such a filter is the "Q", often defined as

$$Q \equiv \frac{\text{resonant frequency}}{\text{3 dB bandwidth}} \tag{4.1}$$

An expression which gives an accurate measure of the Q of a sampled data resonator is [Appendix A]

$$Q = -\frac{|\theta_0|}{2 \ln r_0} \qquad \text{poles at } Z = r_0 e^{j\omega T} \tag{4.2}$$

Using this expression, the locii of poles for a given value of Q can be plotted in the Z plane, as in Figure 4.2a and Table 4.1. It can be seen that, as the pole angle $\theta_0 = \omega_0 T$ increases, the pole radius r_0 required to achieve a given Q, decreases.

A second order transfer function can be written as

$$H(Z) = \frac{N(Z)}{D(Z)} \tag{4.3}$$

where
$$D(Z) = 1 + b_1 Z^{-1} + b_2 Z^{-2} \tag{4.4}$$

$$= 1 - 2r_0 \cos\theta_0 Z^{-1} + r_0^2 Z^{-2} \tag{4.5}$$

and $Z_{1,2} = r_0 e^{\pm j\theta_0}$ are the system poles.

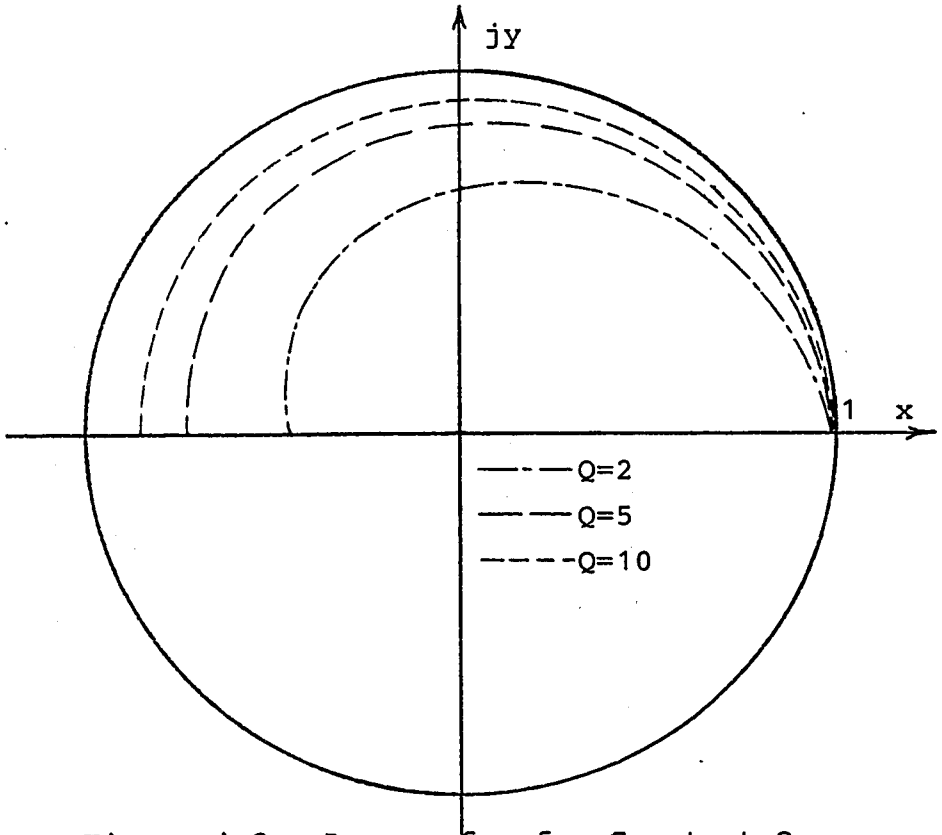

Figure 4.2a Locus of r for Constant Q

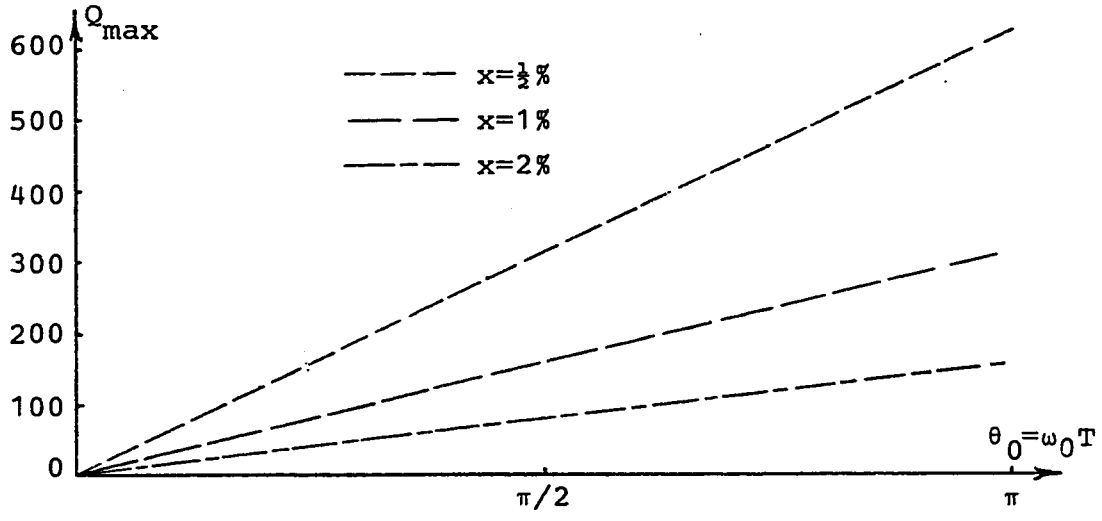

Figure 4.2b Maximum Q Attainable

Figure 4.2 Q Contours

Table 4.1 Pole Radius for a Given Value of Q

θ_0	Q=2	Q=5	Q=10	Q=20	Q=50	Q=100
0	1.000	1.000	1.000	1.000	1.000	1.000
$\pi/4$	.8217	.924	.961	.981	.992	.996
$\pi/2$	.6752	.855	.924	.961	.984	.992
$3\pi/4$	.5549	.789	.889	.931	.997	.988
π	.4559	.730	.855	.924	.969	.984

Gold and Rader[24] have shown that errors in the pole positions caused by inaccuracy in the coefficients b_1 and b_2 are given by

$$\Delta r=\frac{1}{2r_0}\cdot\Delta b_2 \tag{4.6}$$

and $$\Delta\theta=\frac{\Delta b_2}{2r_0^2\tan\theta_0}-\frac{\Delta b_1}{2r_0\sin\theta_0} \tag{4.7}$$

for small Δb_1 and Δb_2. In order to maintain a stable filter, the poles must remain inside the unit circle in the Z plane. Thus if a pole radius can be realized to an accuracy of $\pm\Delta r$, then

$$r_0<1-\Delta r \tag{4.8}$$

for stability. Using the expression for Q,

$$Q=-\frac{|\theta_0|}{2\ln r_0} \tag{4.2}$$

an upper limit for Q can be established,

$$Q_{max}=\frac{-|\theta_0|}{2\ln(1-\Delta r)} \tag{4.9}$$

using a series expansion for $-\ln(1-r)$,

$$Q_{max}=\frac{|\theta_0|}{2(\Delta r+\Delta r^2/2+\Delta r^3/3+\ldots)} \tag{4.10}$$

$$\approx\frac{|\theta_0|}{2\Delta r} \qquad \Delta r<<1$$

$$=\frac{r_0|\theta_0|}{\Delta b_2} \qquad \text{(using 4.6)} \tag{4.11}$$

Assuming that the coefficients b_1 and b_2 can be realized to an accuracy of x%, then

$$|\Delta b_2|_{max} \simeq \frac{x}{100} \qquad r_0 \simeq 1, \quad b_2 \simeq 1 \tag{4.12}$$

and

$$Q_{max} \simeq \frac{100 r_0 \theta_0}{x}$$

$$\simeq \frac{100\theta_0}{x} \tag{4.13}$$

Q_{max} is plotted versus θ_0 for several values of x in Figure 4.2b.

It can be seen that high-Q pole pairs are possible if $r_0 \to 1$ and θ_0 is as large as possible. Large values of θ_0 lead to small separation between the first pass band and the repeated pass band. Values of r_0 close to 1 result in Q being a very sensitive function of b_2. Using the standard definition of Q sensitivity, the expression for $S^Q_{b_2}$ can be found as

$$S^Q_{b_2} = \frac{dQ/Q}{db_2/b_2} = \frac{d \ln Q}{d \ln b_2} \tag{4.14}$$

where

$$Q = -\frac{|\theta_0|}{2 \ln r_0} = -\frac{|\theta_0|}{\ln b_2} \tag{4.2}$$

then

$$\ln Q = \ln|\theta_0| - \ln(-\ln b_2) \tag{4.15}$$

and

$$S^Q_{b_2} = \frac{d \ln|\theta_0|}{d \ln b_2} - \frac{d \ln(-\ln b_2)}{d \ln b_2}$$

$$= 0 - \frac{1}{\ln b_2} \qquad \theta_0 \neq \theta_0(b_2) \tag{4.16}$$

For $b_2 \to 1$, $\ln b_2 \to 0$ and $S^Q_{b_2}$ becomes very large. For $b_2 = .98$ producing a resonator Q of 75, $S^Q_{b_2} = 49.5$. In order to realize the Q to within ±5%, b_2 must be accurate to within ±.01%.

Sensitivity expressions can also be derived for the pole

frequency $\omega_0=\theta_0/T$ with respect to changes in the coefficients b_1 and b_2.

$$\cos\theta_0=-b_1/2r_0=-b_1/2\sqrt{b_2} \tag{4.17}$$
$$-(d\theta_0/db_1)\sin\theta_0=-1/2\sqrt{b_2}$$

then $$S_{b_1}^{\theta 0}=(d\theta_0/db_1).b_1/\theta_0$$
$$=\frac{1}{2\sqrt{b_2}\sin\theta_0}.\frac{b_1}{\theta_0}$$
$$=\frac{b_1}{2\sqrt{b_2}\,\theta_0\sin\theta_0} \tag{4.18}$$

and $$-(d\theta_0/db_2)\sin\theta_0=-(b_1/2)(-\tfrac{1}{2})(1/b_2^{3/2})$$
$$=b_1/(4b_2^{3/2})$$

then $$S_{b_2}^{\theta 0}=(d\theta_0/db_2).b_2/\theta_0$$
$$=-\frac{b_1}{4b_2^{3/2}\sin\theta_0}.\frac{b_2}{\theta_0}$$
$$=-\frac{b_1}{4\sqrt{b_2}\theta_0\sin\theta_0} \tag{4.19}$$
$$=-\tfrac{1}{2}S_{b_1}^{\theta 0}$$

$S_{b_1}^{\theta 0}$ and $S_{b_2}^{\theta 0}$ are large for $\theta_0\to 0$ and $b_2\to 0$; howevever for most cases of interest they are not large. As an example, when $\theta_0=\pi/4$ and $r_0=\sqrt{b_2}=.98$, then $S_{b_1}^{\theta}=1.273$.

Another way of seeing the effect of coefficient error on the filter characteristics is to observe the migration of the poles in the Z plane. Since $b_2=r_0^2$ and $b_1=-2r_0\cos\theta_0=-2y_0$, it is clear that variations in b_2 will cause changes in the pole

radius while variations in b_1 will cause pole shifts parallel to the x-axis. Figure 4.3 illustrates the region bounded by arcs of radius $r_0-\delta r$ and $r_0+\delta r$ and the lines $x=x_0-\delta x$ and $x=x_0+\delta x$, where $\delta r=-\Delta b_2/2r_0$ and $\delta x=\Delta b_1/2$. It is evident that to ensure stability, only b_2 must be controlled, and must be less than 1 in magnitude.

4.3 Effects of CCD Transfer Efficiency

In Chapter two it was shown that substitution of $\frac{\rho Z^{-1}}{1-\varepsilon Z^{-1}}$ for Z^{-1} will model the effect of CCD transfer efficiency on a filter function. As an example, a resonator with poles at $Z=r_0e^{\pm j\pi/2}$ is considered, with $b_1=-2r_0\cos\theta_0=0$. Thus

$$H(Z)=\frac{1}{1+b_2Z^{-2}}=\frac{1}{1+r_0^2Z^{-2}} \tag{4.20}$$

Substitution of $\frac{\rho Z^{-1}}{1-\varepsilon Z^{-1}}$ for Z^{-1} gives

$$\begin{aligned}H'(Z)&=1/\left[1+r_0^2\left(\frac{\rho^2Z^{-2}}{1-2\varepsilon Z^{-1}+\varepsilon^2Z^{-2}}\right)\right]\\&=\frac{1-2\varepsilon Z^{-1}+\varepsilon^2Z^{-2}}{1-2\varepsilon Z^{-1}+\varepsilon^2Z^{-2}+r_0^2\rho^2Z^{-2}}\\&=\frac{1-2\varepsilon Z^{-1}}{1-2\varepsilon Z^{-1}+r_0^2\rho^2Z^{-2}}\qquad(\varepsilon^2<<1)\end{aligned} \tag{4.21}$$

Thus a transfer function zero at $Z=2\varepsilon$ has been created, and the new pole positions are

$$\begin{aligned}Z_{1,2}&=\varepsilon\pm\tfrac{1}{2}\sqrt{4\varepsilon^2-4r_0^2\rho^2}\\&=\varepsilon\pm j\sqrt{r_0^2\rho^2-\varepsilon^2}\qquad\approx\varepsilon\pm j(\rho r_0)\end{aligned} \tag{4.22}$$

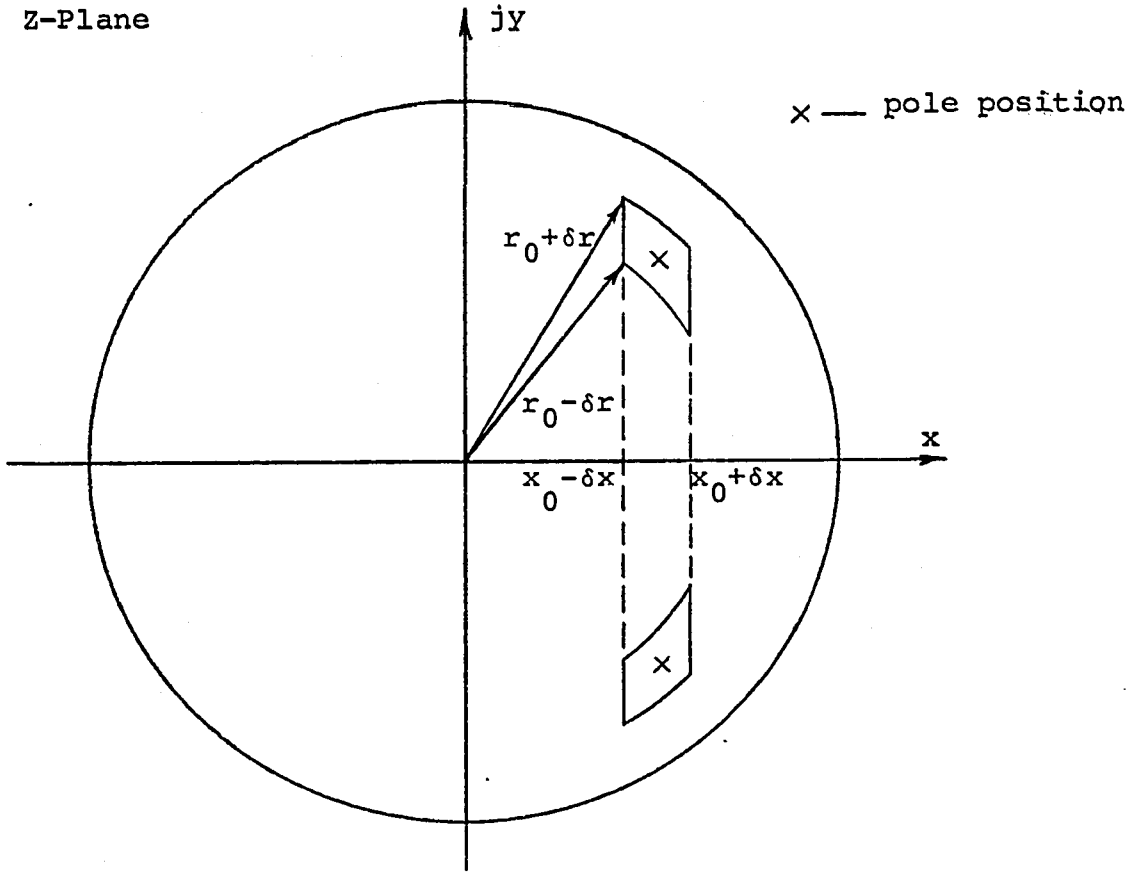

Figure 4.3 Pole Movement Due to Coefficient Error

The poles have been shifted from their intended location at Z $=\pm jr_0$. The pole angle change can be called $\Delta\theta$. Then

$$\tan\Delta\theta=\varepsilon/(r_0\rho)$$
$$\approx\varepsilon/r_0 \qquad (4.23)$$

and for small $\Delta\theta$

$$\tan\Delta\theta\approx\Delta\theta\approx\varepsilon/r_0 \qquad (4.24)$$

For ε on the order of 5×10^{-4} and $r_0\approx1$, the change in pole angle due to charge transfer efficiency would also be on the order of 5×10^{-4}. If $b_1=0$ because of the filter structure, the resonant frequency of the filter would be slightly reduced, and an accurate measure of the deviation from the designed resonant frequency of 1/4T would give a value for ε. For filters with $b_1\neq0$, the effect of coefficient inaccuracy would normally overshadow any effect due to ε.

4.4 Dynamic Range of a CCD Filter

The dynamic range of a given CCD filter will depend upon the requirements of the system of which it is a part. In general, dynamic range can be defined as the ratio between the largest signal capable of being handled by the device or system and the smallest signal which meets some specified criterion, such as a minimum signal to noise ratio. The dynamic range is normally expressed in deciBels. For a CCD filter, the largest signal is usually limited by the

distortion introduced by the filter, which distortion must be less than some set amount. The noise at the output of the filter sets the smallest signal level according to the required signal to noise ratio. This definition of dynamic range will be used in the following chapters.

AN EXPERIMENTAL SECOND ORDER CCD RESONATOR

5.1 Design of a Second Order Resonator

A second order sampled data resonator can be constructed with only one feedback coefficient by setting $b_1=0$, thereby constraining the poles to lie on the imaginary axis in the Z plane, as discussed in Section 4.3 and illustrated in Figure 5.1a. Two, one, or no zeroes can be placed at the origin depending on whether the output of the filter is taken from the second delay stage, the first delay stage, or the adder output respectively (Figure 5.1b). The corresponding transfer functions are

$$H_1(Z)=\frac{z^{-2}}{1+b_2z^{-2}} \tag{5.1}$$

$$H_2(Z)=\frac{z^{-1}}{1+b_2z^{-2}} \tag{5.2}$$

$$H_3(Z)=\frac{1}{1+b_2z^{-2}} \tag{5.3}$$

All three transfer functions have the same frequency magnitude response, and phase responses differing only in the slope corresponding to a constant delay of T or 2T. Figure 5.2 shows the calculated magnitude response for H(Z) with $b_2=.98$. The narrow filter passband is repeated at odd multiples of $\omega T=\pi/2$ due to the sampled data nature of the filter.

A filter was designed to have a Q of 75. From the expression for Q,

$$Q=-\frac{|\theta_0|}{2\ \ln\ r_0} \tag{4.2}$$

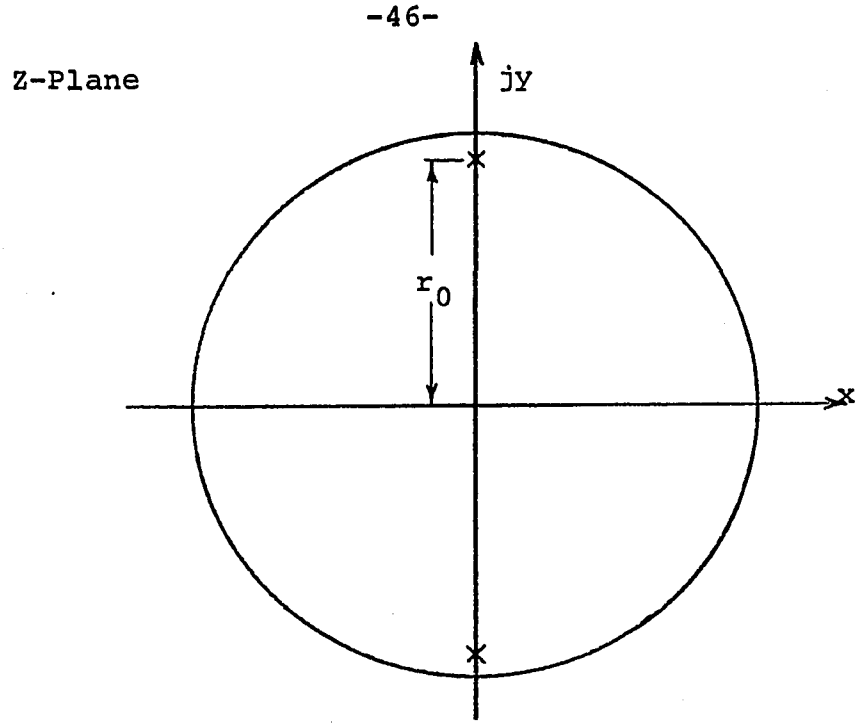

Figure 5.1a

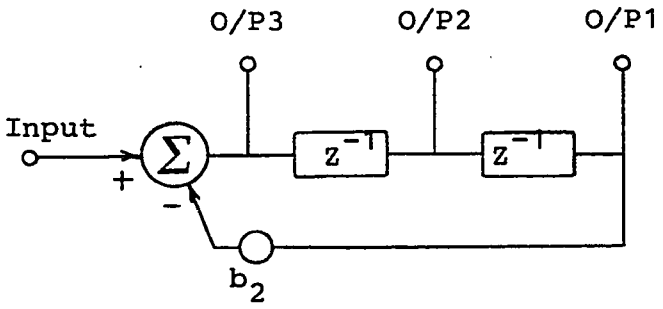

Figure 5.1b

Figure 5.1 Sampled Data Resonator

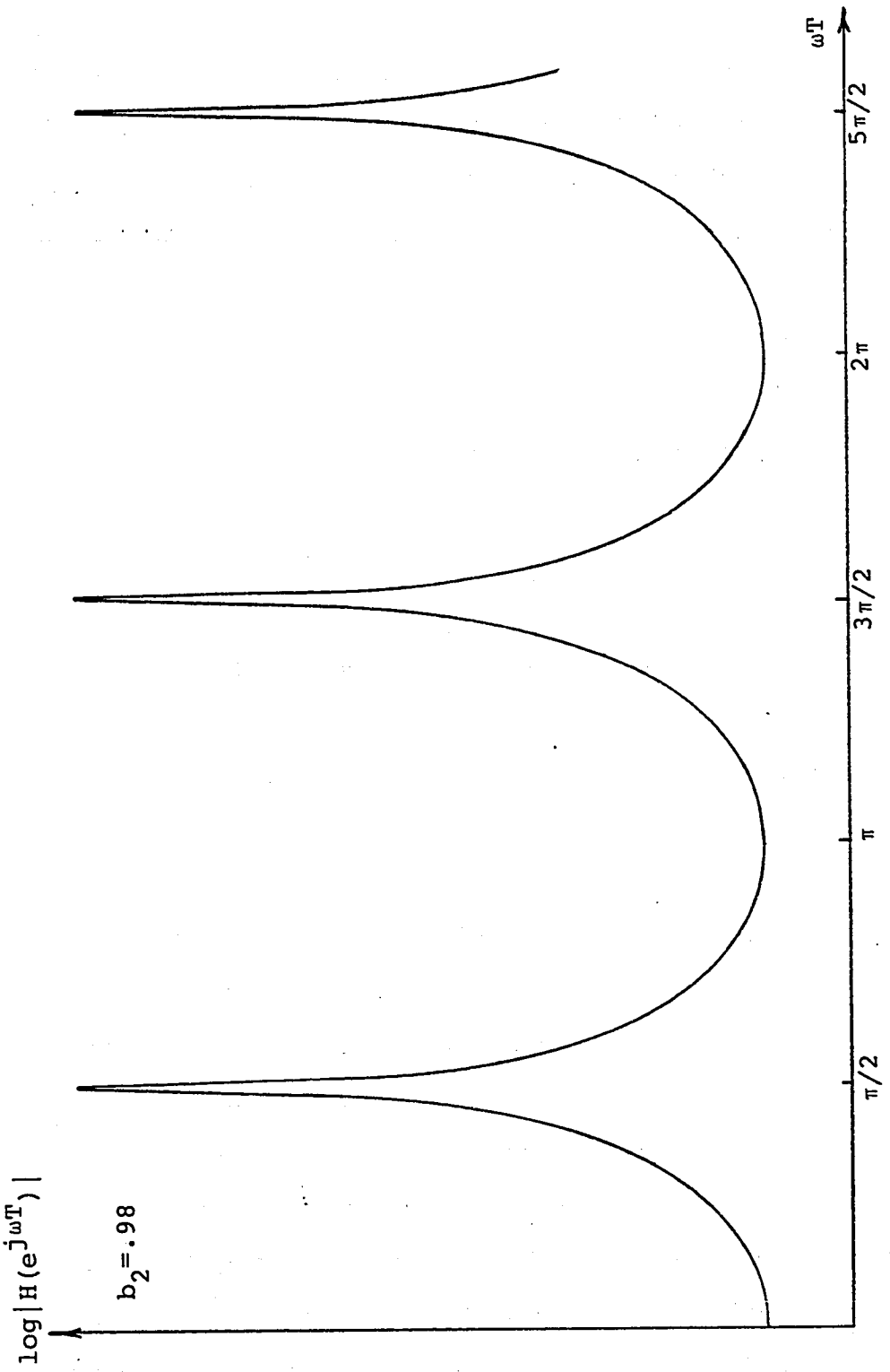

Figure 5.2 Frequency Response of Sampled Data Resonator

is found $$r_0 = e^{-|\theta_0|/2Q} \tag{5.4}$$

Thus in this case for $\theta_0 = \pi/2$, $r_0 = .98958$ and $b_2 = r_0^2 = .97927 \simeq .98$.

An expression relating the minimum and maximum values of the magnitude response to the coefficient b_2 can be derived as follows:

$$|H(e^{j\omega T})|_{max} = |H(e^{j\omega T})|_{\omega T=\pi/2} = \frac{1}{1-r_0^2} \tag{5.5}$$

$$|H(e^{j\omega T})|_{min} = |H(e^{j\omega T})|_{\omega T=0} = \frac{1}{1+r_0^2} \tag{5.6}$$

$$\frac{|H(e^{j\omega T})|_{max}}{|H(e^{j\omega T})|_{min}} = \frac{1+r_0^2}{1-r_0^2} \tag{5.7}$$

or $$b_2 = r_0^2 = \frac{|H(e^{j\omega T})|_{max} - |H(e^{j\omega T})|_{min}}{|H(e^{j\omega T})|_{max} - |H(e^{j\omega T})|_{min}} \tag{5.8}$$

5.2 A CCD Realization of a Second order Resonator

Figure 5.3 shows the realization of the resonator using the ten stage CCD delay line described in Chapter two. A portion of the output from stage 2 is taken from the potentiometer slider, a DC bias is added to it, and this signal is subtracted from the filter input by the CCD input stage. Measurement of the feedback coefficient b_2 directly was difficult to perform to an accuracy of better than about 2%. Consequently b_2 was calculated from the frequency response plot using equation 5.8. Figure 5.4 is a frequency response plot of the filter for a clock rate (sampling frequency) of 40 kHz. The value of b_2 calculated from the maximum and minimum

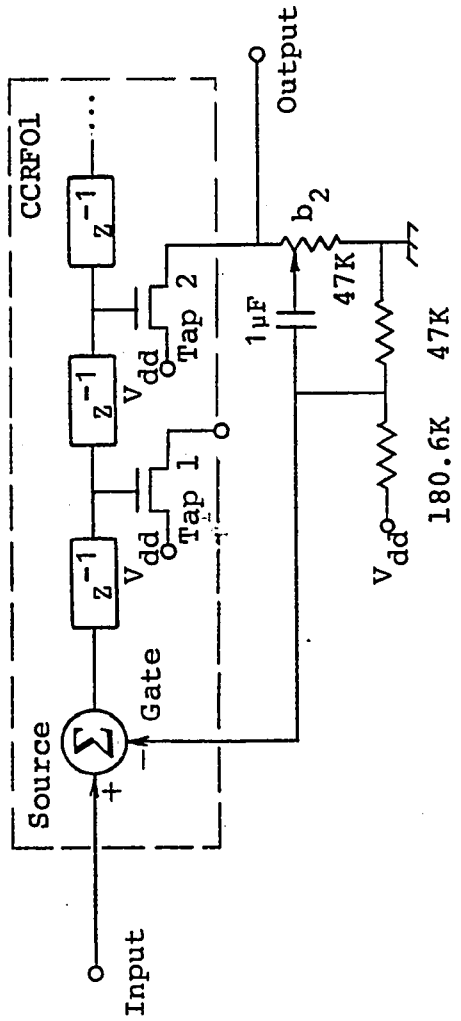

Second Order CCD Resonator

Figure 5.3 CCD Second Order Resonator

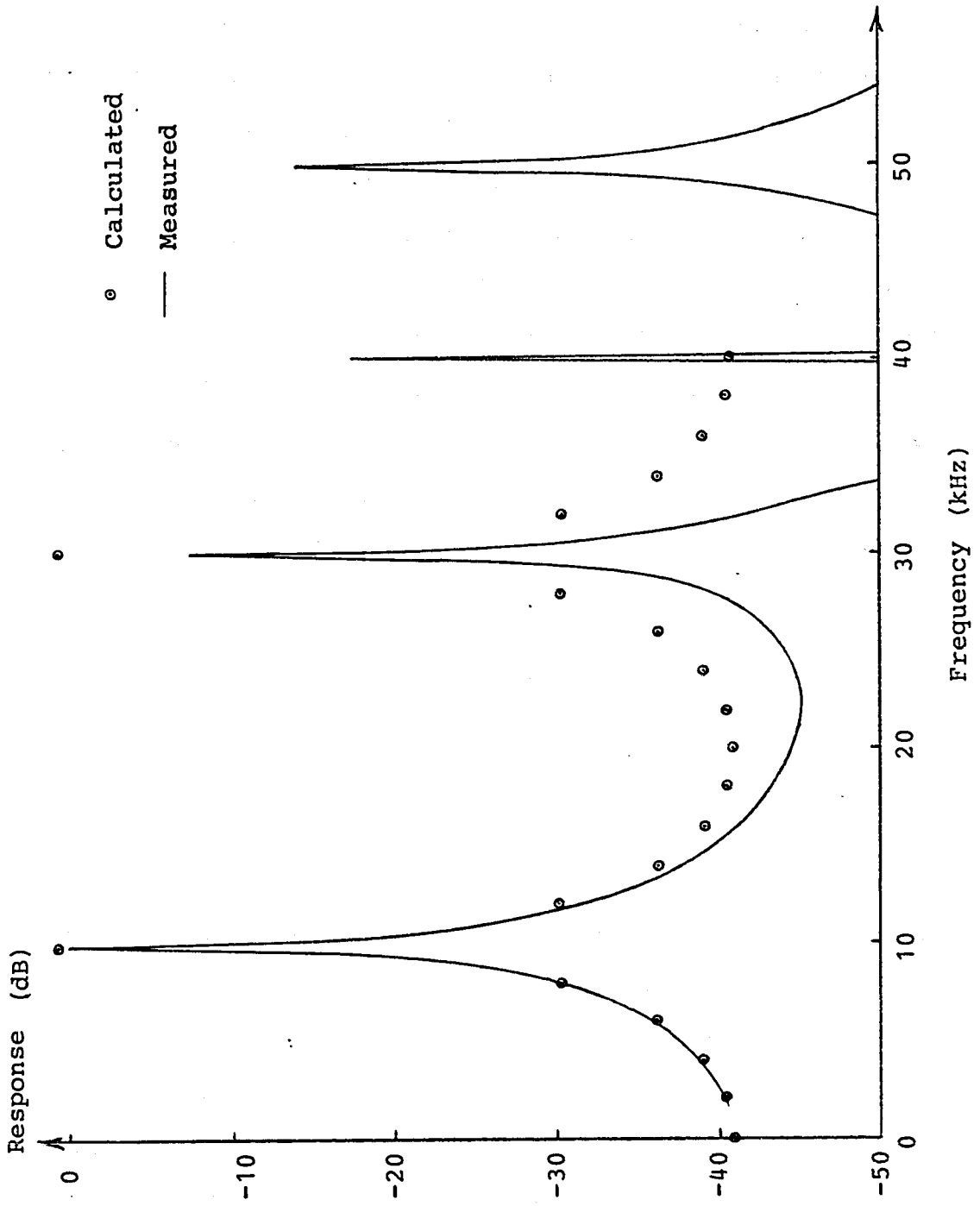

Figure 5.4 CCD Resonator Frequency Response

values of the response is .9839. Also plotted in Figure 5.4 is the calculated frequency response of a filter with a value of b =.9839. The $\frac{\sin \omega T/2}{\omega T/2}$ rolloff of the measured response due to the output sample and hold circuit is evident.

Figure 5.5 shows the output noise spectrum of the filter with the input grounded, measured with a wave analyzer bandwidth of 100 Hz (equivalent ideal filter bandwidth =120 Hz). The sharp peak in the spectrum at the filter resonant frequency indicates that the noise must originate at the filter input, since the noise spectrum has been filtered. The 0^{dB} level of the graph is normalized to the filter peak output level for an input signal level of 3mV RMS. At the resonant frequency, this filter provides a gain of

$$|H(e^{j\omega T})| = \frac{1}{1-r_0^2} \qquad (5.5)$$

$$= \frac{1}{1-.9839}$$

$$= 62.1$$

Consequently the input signal must be small enough that the CCD is capable of handling an output signal which is 62.1 times as large. This reduces the dynamic range of this type of filter as compared to a transversal filter, which does not require that an enlarged output signal be fed back through the CCD. Lower-Q resonators would have increased dynamic range.

An attempt was made to measure the exact frequency at which the peak response occurred, in order to evaluate the

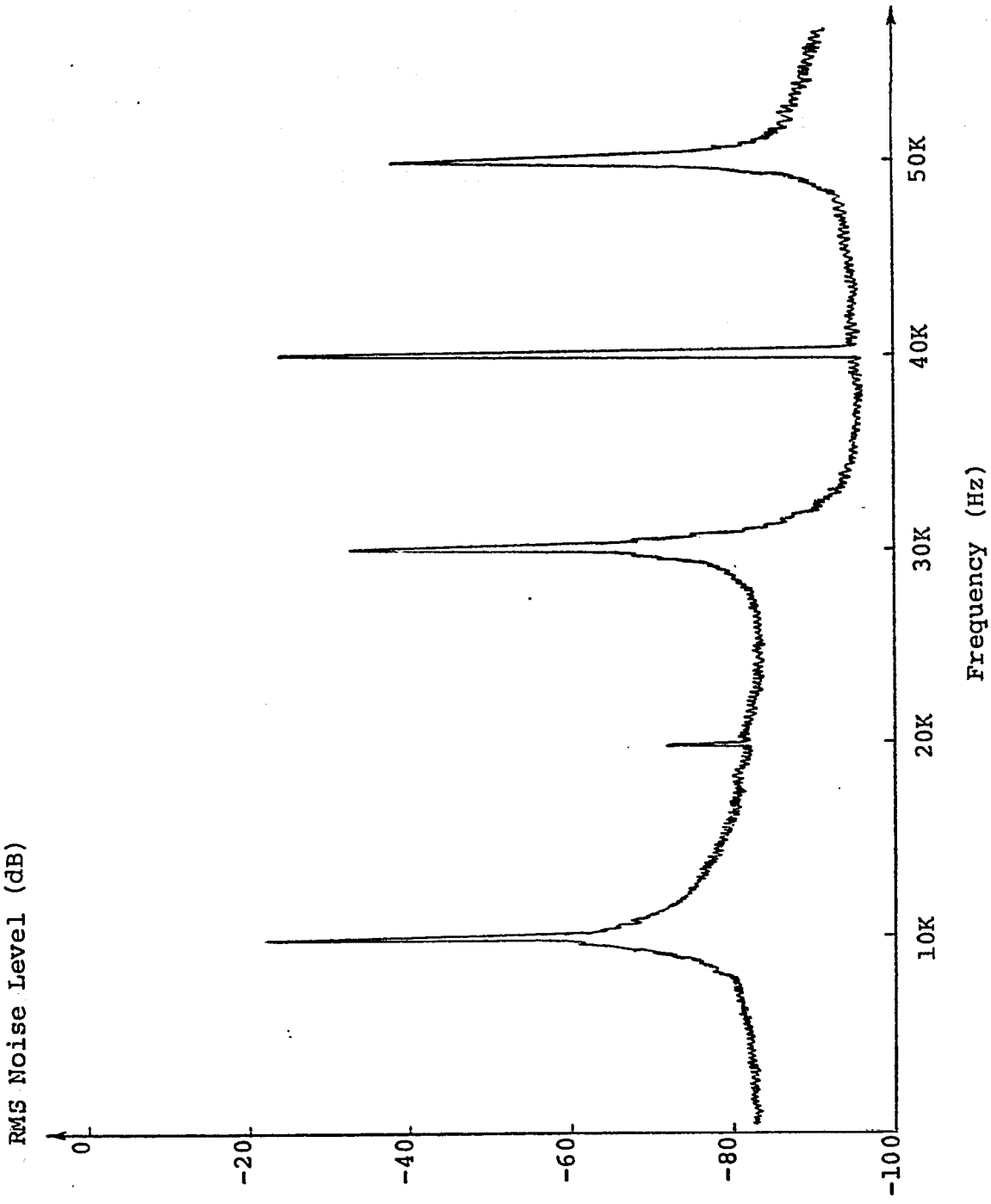

Figure 5.5 Filter Output Noise

transfer efficiency ε as described in Chapter four. The peak, however, has a flat top and it was difficult to measure the resonant frequency. A more sensitive method would be to observe the phase shift of the output signal, since the phase changes rapidly with frequency.

AN EXPERIMENTAL SECOND ORDER CCD FILTER SECTION

6.1 Design of a General Second Order CCD Filter Section

A complex conjugate pair of poles and a complex conjugate pair of zeroes in the Z plane can be realized by a general second order section. The frequency response of such a section will peak at a frequency ω_{max} near the pole frequency ω_p (where $\theta_p=\omega_p T$ is the pole angle), and have a minimum at ω_{min} near the zero frequency ω_z. If the zeroes lie on the unit circle, then $\omega_{min}=\omega_z$ and the frequency response has a null at that frequency. Sections may be cascaded to realize a transfer function of any order. Chapter seven discusses how second order sections are used to realize a fifth order elliptic function lowpass filter. Such filters have transfer function zeroes on the unit circle, causing nulls in the stop band. The response of a typical second order section, showing the frequencies of interest, is given in Figure 6.1.

Of the low pass filter to be described in Chapter seven, the section having the highest Q pole pair and the zero pair closest to the filter cutoff frequency was first chosen for CCD realization. For this section the pole and zero locations are as follows:

$$Z_{p1,p2}=.9391153e^{\pm j.6664880} \quad \text{(poles)}$$

$$Z_{z1,z2}=1.0000000e^{\pm j.8994701} \quad \text{(zeroes)}$$

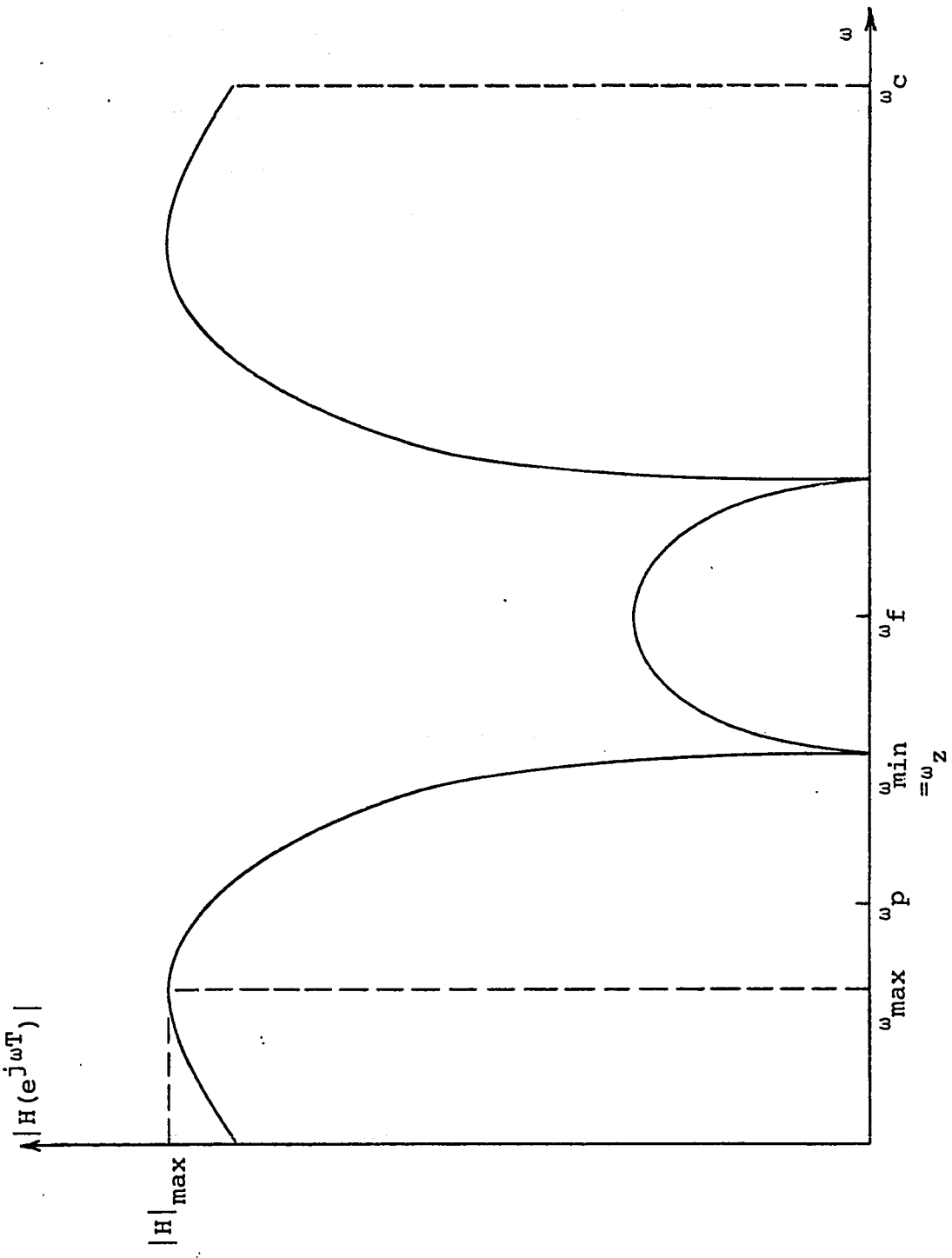

Figure 6.1 Second Order Section Frequency Response

The transfer function is then

$$H(Z)=\frac{1.00000-1.24405Z^{-1}+1.00000Z^{-2}}{1.00000-1.47629Z^{-1}+0.881938Z^{-2}}$$

The computed frequency magnitude response of the section is shown in Figure 6.2. No scaling factor has yet been applied; consequently the peak has a value

$$|H(e^{j\omega T})|_{max}\approx 13.34 \text{ dB}$$
$$\approx 4.645$$

Thus an input sinusoid at a frequency $\omega=\omega_{max}$ (corresponding to $|H(e^{j\omega T})|_{max}$) is enlarged by a factor of 4.645 at the output of the section. Consideration must be given to ensuring that the cascade of sections produces the desired overall filter gain, normally unity in the pass band; this will be discussed in Chapter seven.

In Figure 6.3 a block diagram is shown of the general second order section. The signal w(nT), which passes through the CCD channel, must be scaled so that its amplitude does not exceed the signal handling capability of the CCD. By inspection,

$$w(nT)=x(nT)-b_1w(nT-T)-b_2w(nT-2T) \qquad (6.2)$$

$$W(Z)=X(Z)-b_1W(Z)Z^{-1}-b_2W(Z)Z^{-2} \qquad (6.3)$$

$$H'(Z)=\frac{W(Z)}{X(Z)}=\frac{1}{1+b_1Z^{-1}+b_2Z^{-2}} \qquad (6.4)$$

The input signal x(nT) appears as w(nT) at the adder output modified by a transfer function consisting of the denominator

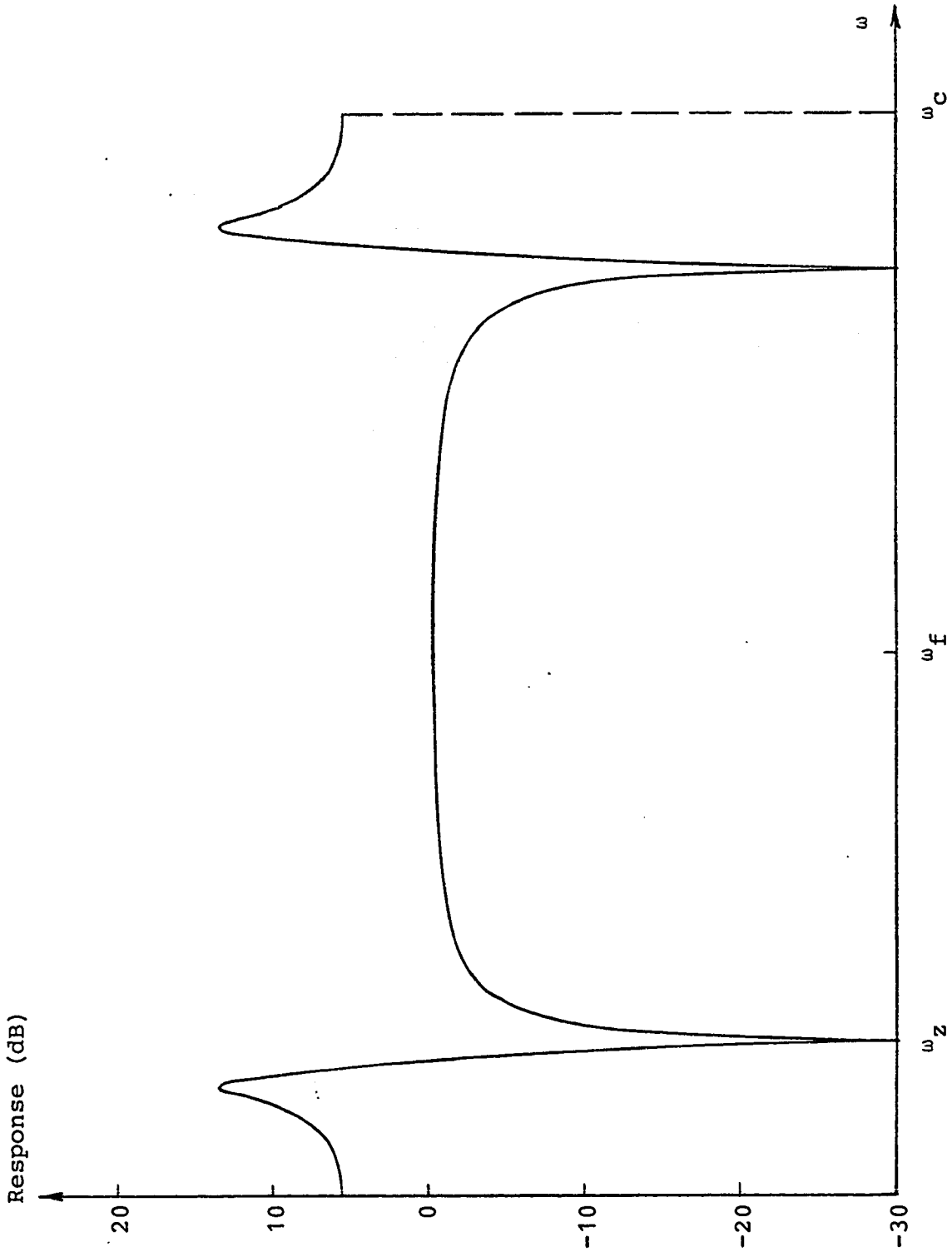

Figure 6.2 Computed Frequency Response of H(Z)

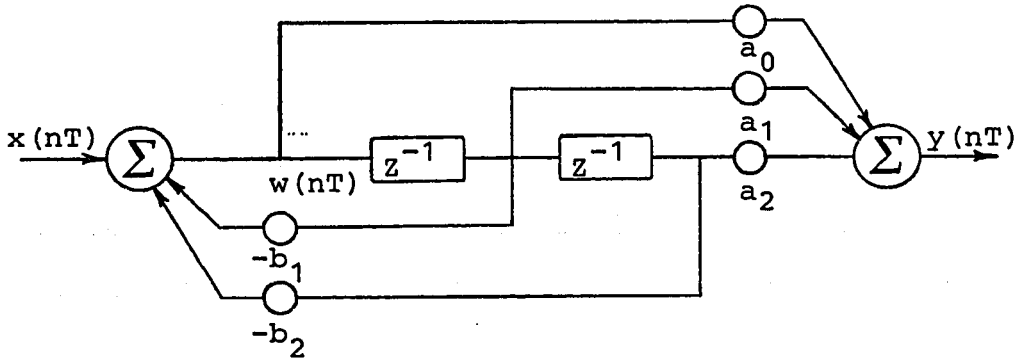

Figure 6.3 General Second Order Section

only of the section transfer function H(Z). The magnitude response of H'(Z) is given in Figure 6.4. An input signal $x(t)=A\sin\omega_{max}t$ must be 22.64 dB below the peak signal handling ability of the CCD. For the CCD's used in this work, a maximum peak to peak signal level of .7 Volts could be handled; consequently x(t) must have a value of .052 Volts peak to peak. A voltage divider is required to reduce the input signal to this level. The overall gain of the section is adjusted by scaling the feedforward coefficients by a constant factor.

6.2 A CCD Realization of a General Second Order Section

The second order section presented in Section 6.1 has been realized using five stages of the ten stage, voltage sensed CCD described in Chapter two. The staggered arrangement of feedforward and feedback terms described in Chapter four is used. The filter implementation is shown in Figure 6.5. Three operational amplifiers provide the weighting and summation of the feedback terms, the input signal and a DC bias for the CCD. The feedforward terms are weighted and summed by a second set of three operational amplifiers, the output of which is sampled and held, then buffered by a voltage follower to produce the filtered output.

Figure 6.6 is a plot of the measured frequency response of the filter section. The clock frequency is 24 kHz. The

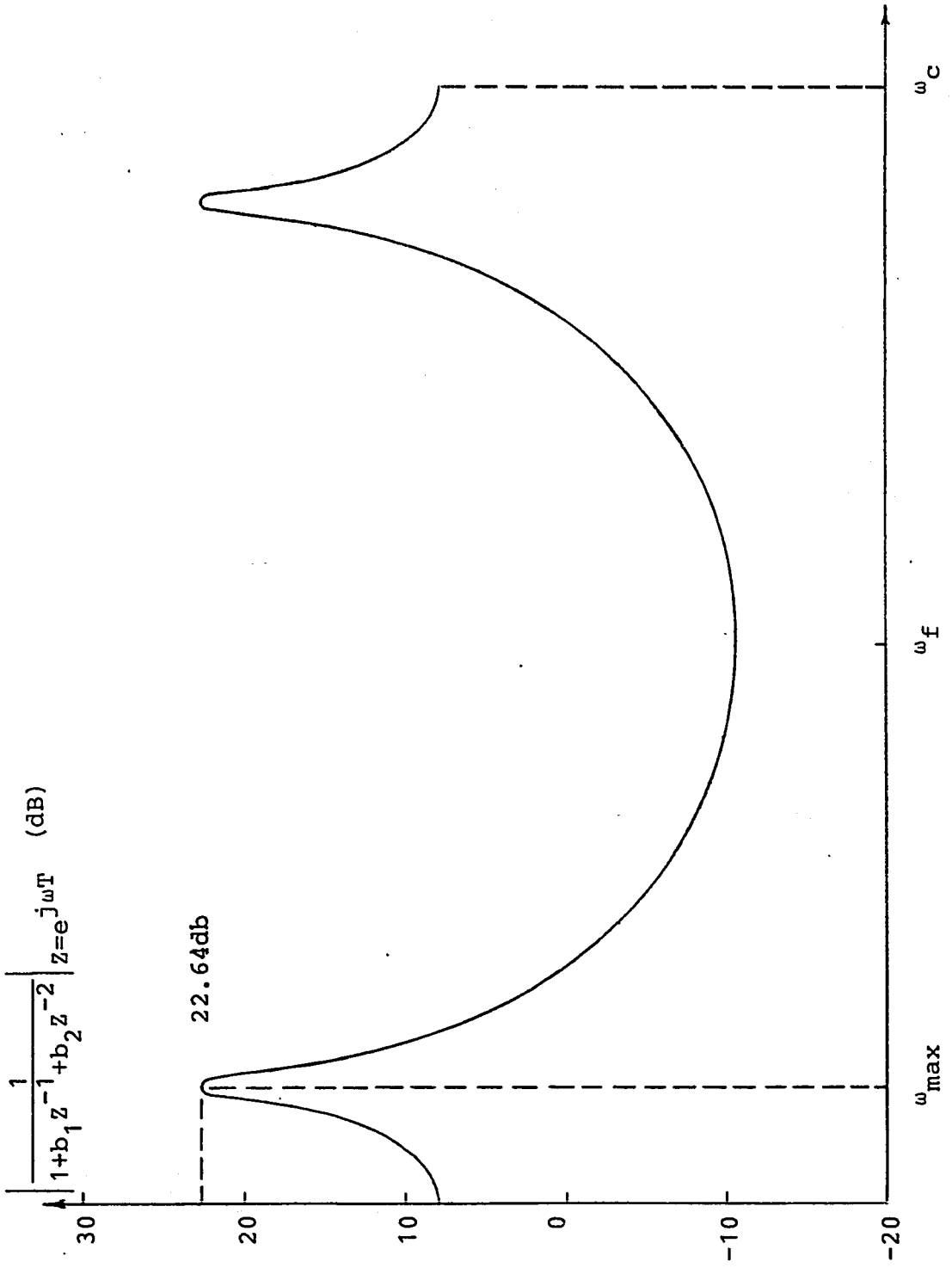

Figure 6.4 Frequency Response of $\left|\frac{1}{1+b_1z^{-1}+b_2z^{-2}}\right|$

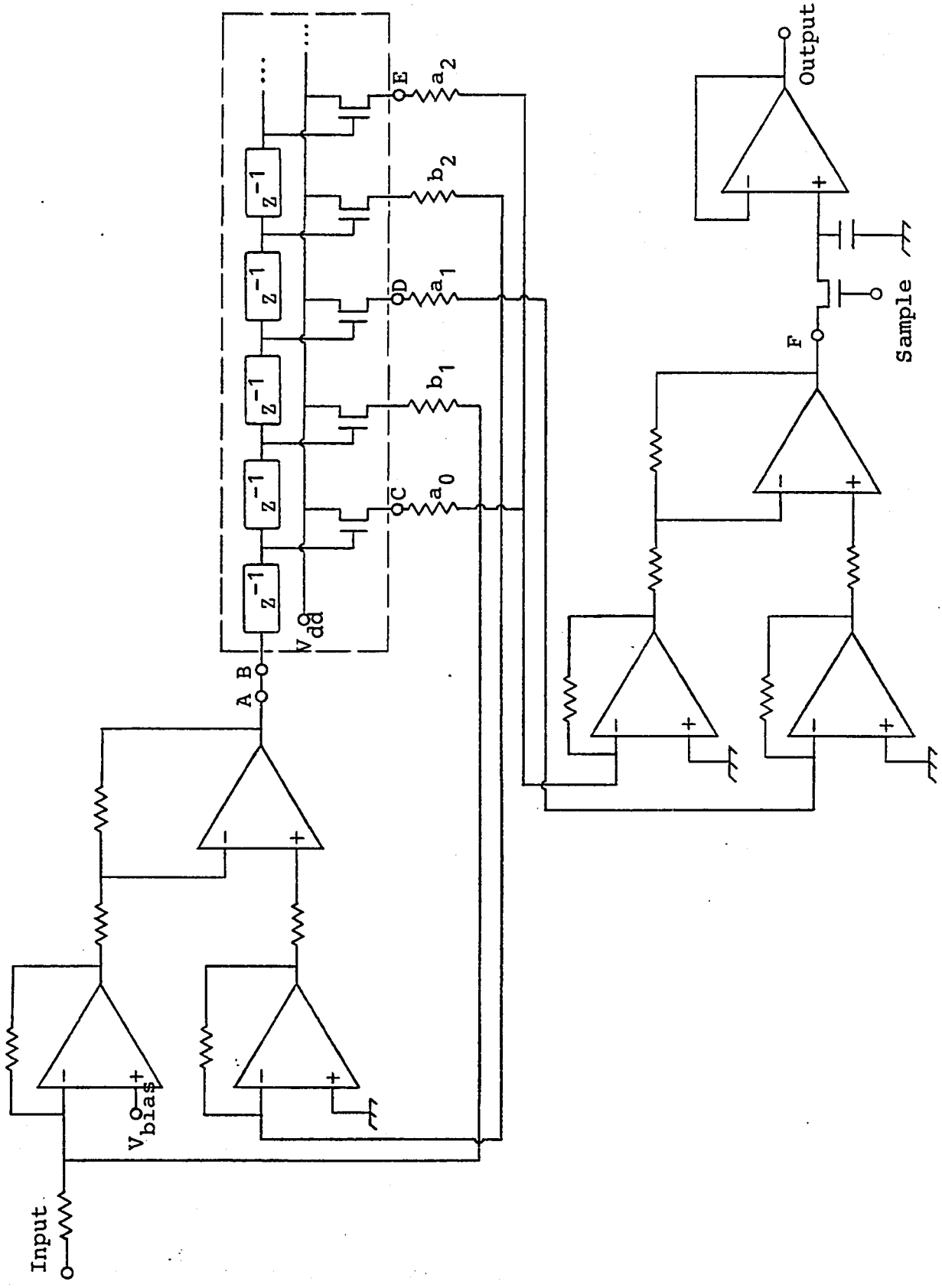

Figure 6.5 CCD Implementation of General Second Order Section

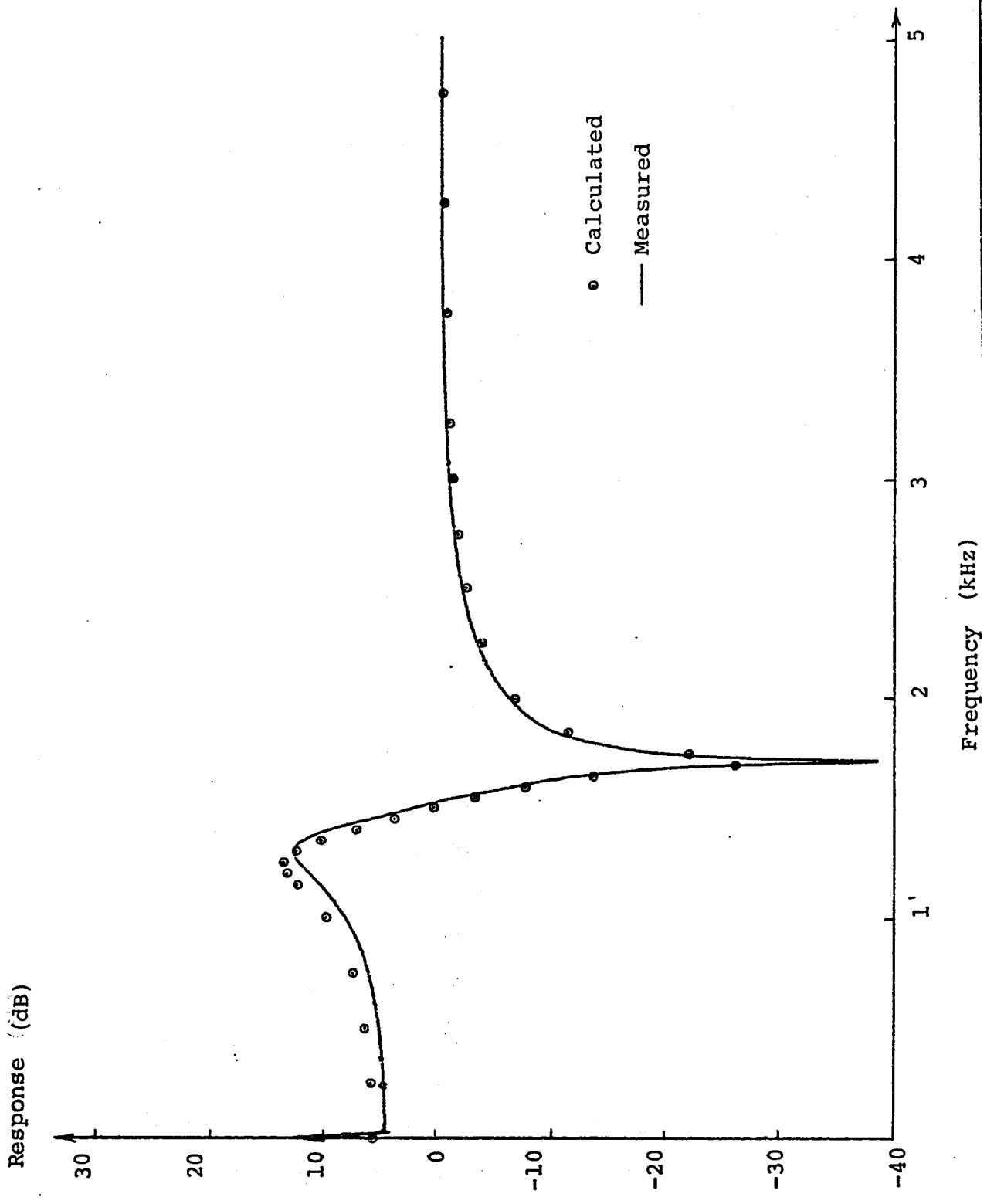

Figure 6.6 Frequency Response of Second Order Filter

measured response agrees closely with the calculated values for frequencies higher than 1.8 kHz; below this the response peak is about .5 dB lower than it should be and ω_{max} is about 63 Hz higher than the design value. Using the sensitivity formulae of Chapter four indicates that both $|b_1|$ and $|b_2|$ are low by approximately 3%. This is the estimated accuracy to which the feedback coefficients could be set using an oscilloscope. The method of measurement was to break the link between points A and B in Figure 6.5, apply a sinusoidal voltage with an appropriate DC bias to point B, and measure the response at point A for the b_1 and b_2 weighting resistors connected in turn. The feedforward coefficients, which realize the zeroes of the filter section, produce a sharp null in the frequency response at almost exactly the correct frequency, indicating very little coefficient error. These coefficients were measured by introducing a sinusoidal voltage at points C, D, and E of Figure 6.5 in succession, and measuring the response at point F with an RMS voltmeter. The estimated accuracy for these measurements was ±.5%.

Figure 6.7 shows the measured frequency response of the section, for frequencies from 0 to 50 kHz. The repeated response shape due to the sampling process is clearly seen, as is the $\frac{\sin\omega T/2}{\omega T/2}$ envelope caused by the holding of the output samples from one sampling instant to the next. The folding frequency $\omega_f/2\pi$ occurs at 6 kHz on account of the two stages of delay between adjacent feedforward or feedback taps.

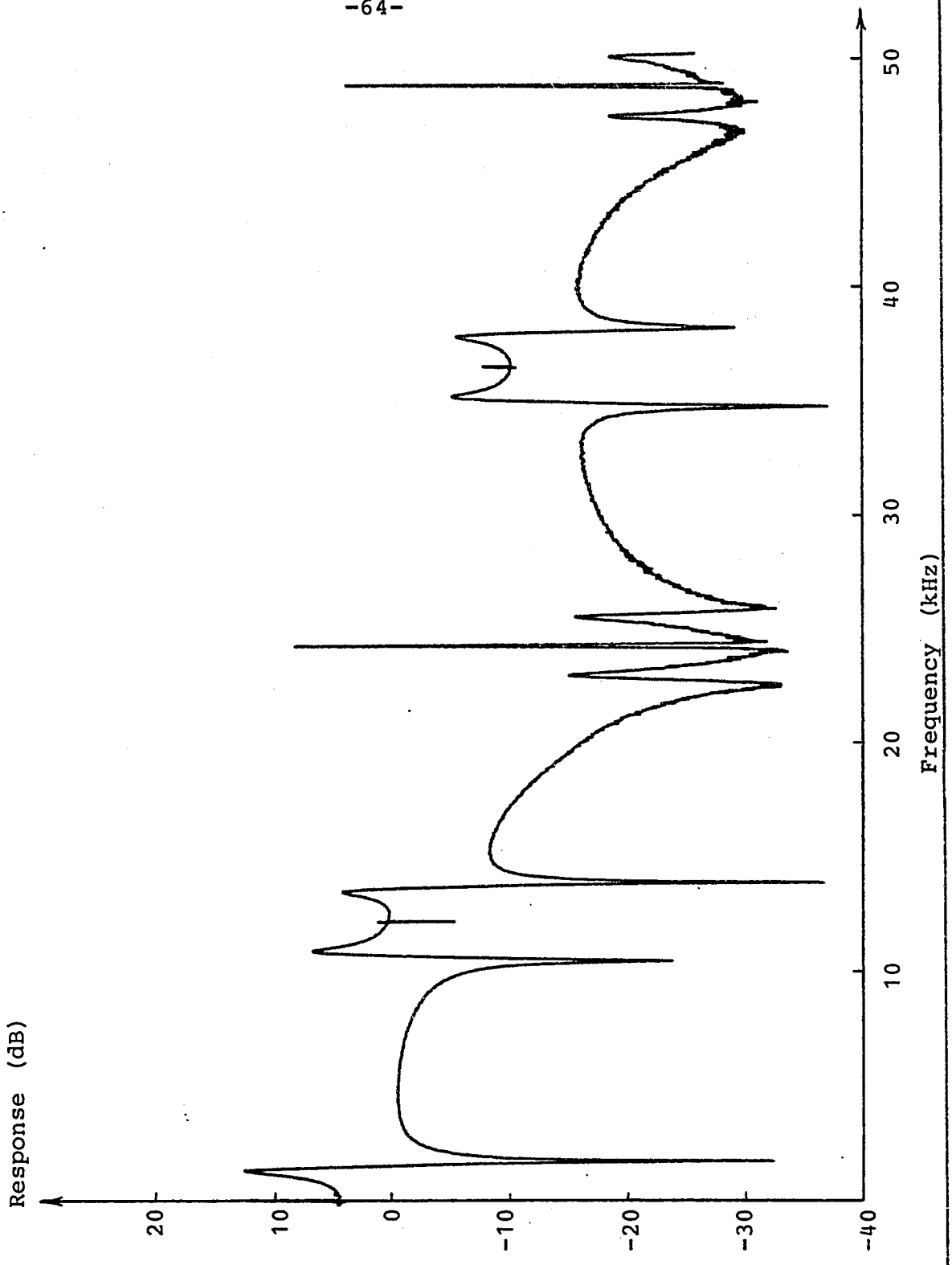

Figure 6.7 Frequency Response Showing Folding

Noise at the output of the section, measured in a 30 Hz spectrum analyzer bandwidth (36 Hz ideal filter bandwidth), is plotted in Figure 6.8. The vertical axis is normalized to the same scale as in Figure 6.7. The level of the first noise "spike" is 42 dB below the maximum output level of the section. The spikes occur at harmonics of the power line frequency, specifically at the third, fifth and ninth harmonics for the most noticeable spikes. A careful attempt at eliminating ground loops in the interconnecting wiring reduced the noise from a much higher level to the level shown. The remainder of the power line related noise was probably coupled through the clock pulse leads, modulating the size of the CCD charge packets.

The expected relative gain error of the analyzer used in these measurements and in those of Chapter 7 is specified as $\pm$ 0.25 dB/dB but not more than $\pm$ 1.5 dB over a 70 dB range. The frequency response of the analyzer using its own tracking generator was flat to within the resolution of the display.

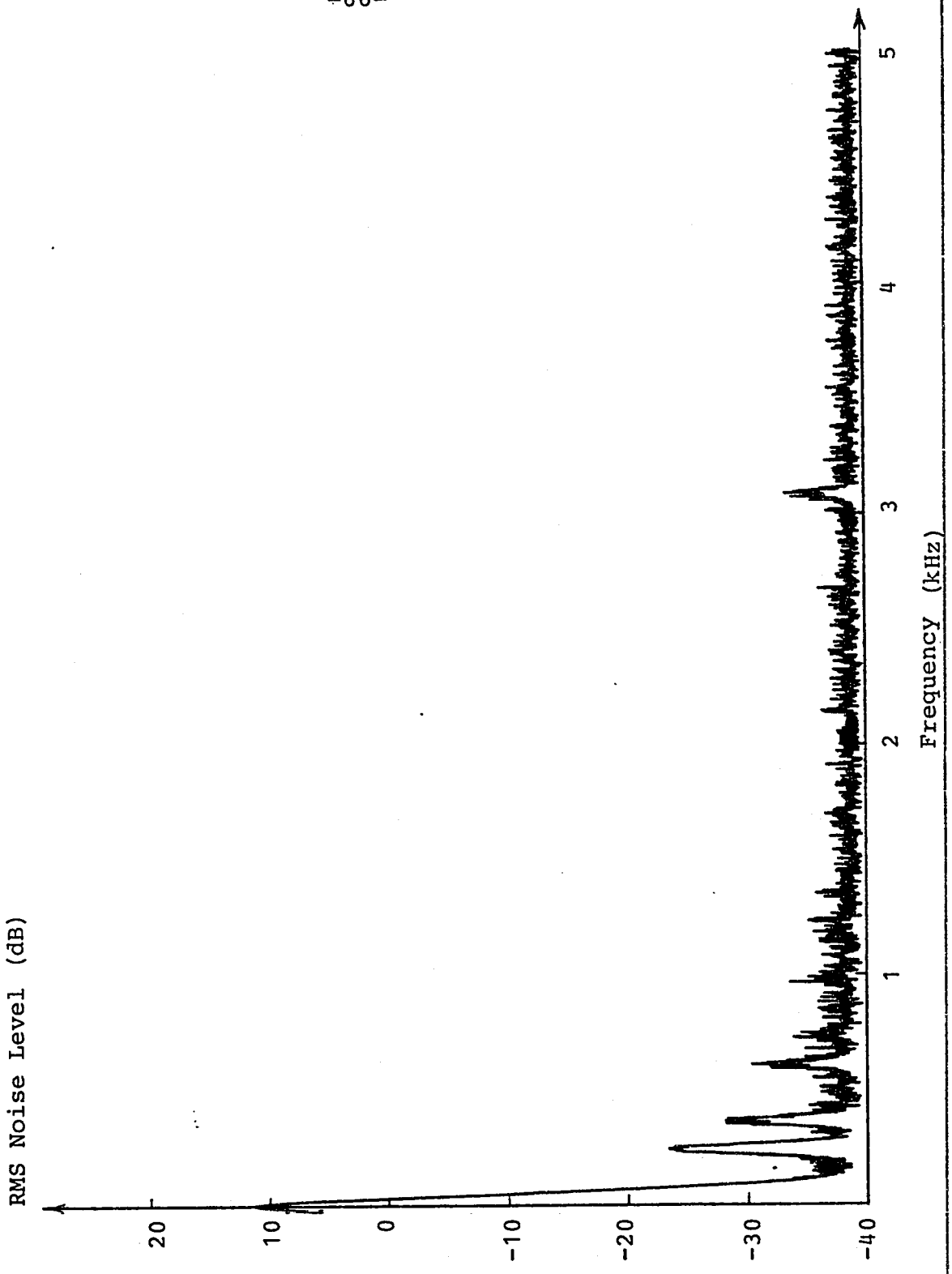

Figure 6.8 Output Noise Spectrum

AN EXPERIMENTAL FIFTH ORDER CCD LOWPASS FILTER

7.1 Selection of Pole-Zero Pairs, Scaling, and Ordering of a Cascade of Sections

A filter of order N made up of a cascade of second order sections, and a first order section for N odd, has a total of M=N/2 (N even) or M=(N+1)/2 (N odd) sections. The designer is normally free to choose which pair of zeroes will be grouped with a pair of poles, and in which order the sections will be realized. A total of M! pole-zero pairings and M! section orderings are possible, producing a total of $(M!)^2$ different realizations for N even, and M!(M-1)! different realizations for N odd. For digital filters, a common procedure to find an optimum (in one sense) realization is to find the structure which has the minimum ratio of maximum to minimum in-band magnitude response at all summing junctions, and to scale the response at each junction so that the maximum expected level is almost equal to the maximum arithmetic capacity of that adder[25,26]. A filter in which the accuracy to which the coefficients can be implemented does not change with the filter structure, has a transfer function sensitivity $S_{\gamma i,j}^{H(j\omega)}$ which is independent of pole-zero pairing and section ordering. This can be seen by noting that all of the $(M!)^2$ or M!(M-1)! possible structures can be found by merely reordering the second order numerator and denominator factors

of the transfer function H(Z). For external coefficient weighting using operational amplifiers, as was done in this work, the coefficient errors of one section are not dependent on those of any other section, and the feedforward coefficients of any one section are not related to the the feedback coefficients of that section. Thus any pairing and ordering could be considered without regard to changing the transfer function sensitivity.

For CCD implementation of sampled data filters, primary consideration must be given to the signal handling capability of the CCD. Thus, as seen in Chapters five and six, the maximum input signal to the CCD must not exceed a given peak to peak value. For $D_i(Z)$ the denominator of $H_i(Z)$,

$$\frac{W_i(Z)}{X_i(Z)} = \frac{1}{D_i(Z)} \qquad i=1,2,\ldots,M$$

The maximum value of $\left|\frac{1}{D_i(e^{j\omega T})}\right|$ must be scaled to the CCD operating range by multiplying the input signal $x_i(nT)$ by a scaling factor p_i. Figure 7.1 shows a fifth order cascade filter incorporating scaling coefficients p_i. Considerable savings in hardware can be achieved by incorporating the p_i into the feedforward coefficients of the preceeding section, ie

$$\alpha'_{i,j} = \frac{\alpha_{i,j}}{p_{i+1}} \qquad i=1,2,\ldots,M-1$$

and by making the output adder of each section contiguous with the input adder of the next section. These changes are shown

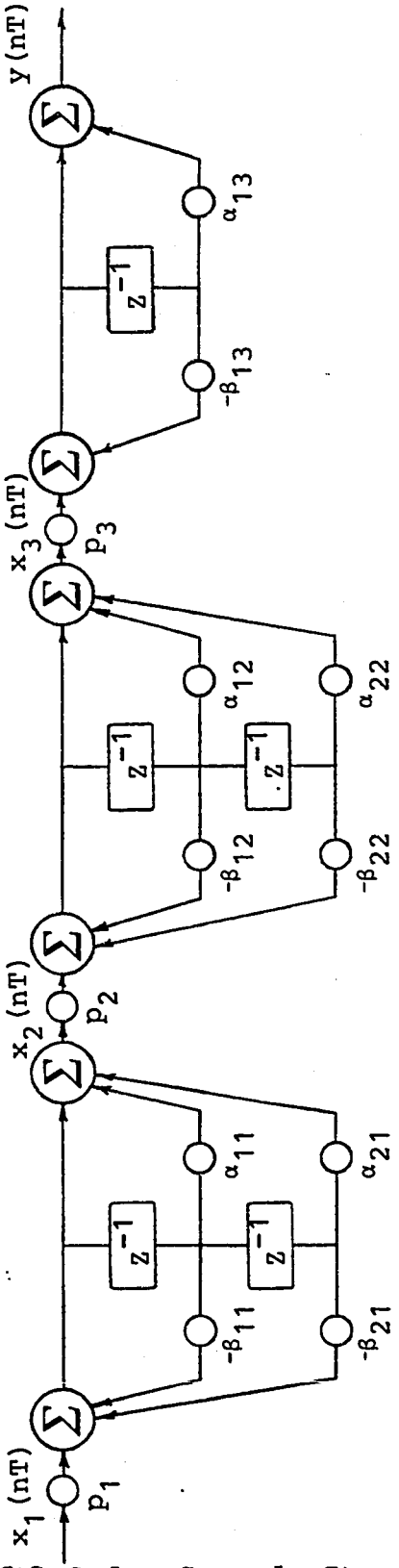

Figure 7.1 Fifth Order Cascade Structure

in Figure 7.2. The feedforward coefficients of the last section can be scaled to give the filter any desired pass band gain.

The criterion used in this work for the pairing of poles and zeroes is that the ratio of the maximum to the minimum in-band magnitude response for each section be a minimum. For a low pass filter, the pole pair nearest the filter cutoff frequency is taken with the first zero pair in the stop band; the adjacent pole pair with the next zero pair, and so on. This procedure ensures that the section with the pole pair causing the largest amount of "peaking" in the frequency response (ie the highest Q poles) has its peaking tendencies reduced as much as possible. Thus the input to the succeeding section is as large as possible for all frequencies in the filter pass band, and the signal to noise ratio is at a maximum.

Ordering of the sections of the low pass filter to be described was somewhat arbitrarily done by placing the highest Q pole pair section first, followed by the next highest Q pole pair section, and then the first order section. It was felt that with the reverse ordering, the high Q pole pair section (the one with the most gain) would amplify all of the noise from the preceeding sections as well as its own noise contribution, producing a larger total noise output. Once the ordering has been decided upon, an improvement in the scaling can be achieved. Originally the scaling factors p_i were chosen

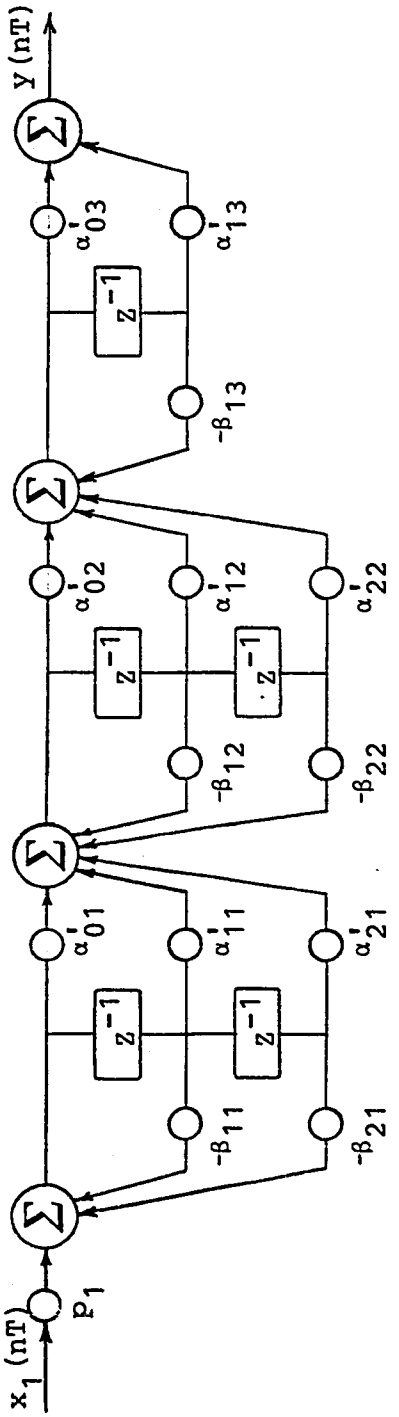

Figure 7.2 Modified Fifth Order Cascade Structure

to limit the peak response of each section, assuming an input signal of constant amplitude across the frequency range of interest. For the second and any succeeding sections, however, the input signal has been prefiltered by the preceeding sections. Thus a better way of scaling for the second section, for example, is to scale for the maximum value of

$$\left| \frac{N_1(e^{j\omega T})}{D_1(e^{j\omega T})} \cdot \frac{1}{D_2(e^{j\omega T})} \right|$$

which is the frequency response of the first section and the recursive part only of the second section.

7.2 Design of an Elliptic Function Lowpass Filter

A low pass filter for voice-band filtering applications, is designed to meet the following criteria:

pass band ripple	.1 dB
stop band attenuation	>35dB
transition ratio	.75
cutoff frequency	3200 Hz
clock frequency	32000Hz

The order N=5 is found sufficient to meet these requirements. The minimum stop band attenuation is 40 dB. Bilinear transformation of the analog design (using the method of Section 3.4) yields the following Z plane pole and zero locations:

$1.000000e^{\pm j.89947013}$ (zero pair)

$1.000000e^{\pm j1.2424260}$ (zero pair)

$1.000000e^{\ j3.1415927}$ (single zero)

$.9391153e^{\pm j.6664880}$ (pole pair)

$.7765535e^{\pm j.5106619}$ (pole pair)

$.6441190e^{\ j0.0}$ (single zero)

Pairing of the poles and zeroes and scaling of each section according to the method described in Section 7.1, produces the following coefficients:

$p_1=.11130$

$p_2=.29274$

$p_3=.537057$

Section 1 $a_0'=.29274$

$a_1'=-.36418$

$a_2'=.29274$

$b_1=1.47629$

$b_2=-.881938$

Section 2 $a_0'=.537057$

$a_1'=-.346403$

$a_2'=.537057$

$b_1=1.35496$

$b_2=-.603035$

Section 3 $a_0=1.00000$

$a_1=1.00000$

$b_1=.644119$

A Monte Carlo analysis program determines what effects random coefficient errors up to a certain maximum value have on the frequency response of the filter. For maximum coefficient errors of .2% and .1% the pass band ripple increases to about .65 dB and .35dB maximum respectively from the design value of .1 dB, while the stop band response remains virtually unchanged. This increase in the pass band ripple must be taken into account in the filter design process.

A method of reducing the effect of coefficient error on pass band ripple is to increase the filter order. Methods have been presented in the literature for reducing the Q of the highest Q poles of Butterworth[27] and Chebyshev[28] filters. These methods involve adding pole pairs while maintaining, as far as possible, the same filter specifications as in the original. For elliptic function filters there are four frequency response variables, three of which must be specified;

N - filter order

D_p - pass band ripple

D_a - minimum stop band attenuation

k - transition ratio $=\omega_p/\omega_s$

If the order N is increased, while k and D_a are held constant, then D_p is reduced. As an example, two filters, one sixth order and

the other seventh order, were designed to meet the requirements

$k=0.75$

$D_a=52$ dB

resulting in $D_p=0.2$ dB for N=6 and $D_p=0.01$ dB for N=7. When transformed to the Z plane by means of the bilinear transformation so that $\omega_p T=2\pi/10$, the Q of the highest Q pole pair is 9.0 for N=6 and 8.4 for N=7. Subjecting the filters to a Monte Carlo analysis produces the results of Table 7.1.

Maximum Coefficient Error	N=6	N=7
.1%	1 dB	.16 dB
.2%	1.9 dB	.32 dB

Table 7.1 Maximum Passband Ripple Due to Coefficient Error

A considerable improvement in the maximum pass band ripple is obtained by increasing the order of the filter by only one. More improvement might be expected by further increasing the filter order, at the expense of greater circuit complexity. This could be confirmed by using computer filter design programs.

7.3 Realization of a CCD Elliptic Function Low Pass Filter

The fifth order low pass filter design of Section 7.2 was realized using three CCD's, two of which performed second order filtering functions and the third a first order

function. Operational amplifiers were used for the coefficient weighting and summing. Figure 7.3 shows the filter layout. The bias voltages set the DC levels of the input signals to the CCD's. The output signal is taken via a sample and hold circuit and a voltage follower. All of the coefficient weighting resistors were accurately preset by using a digital ohmmeter. The potentiometer at the input to each section was then adjusted to compensate for the CCD gain, by observing the frequency response of each section. Most of the coefficient error can be attributed to this second step, since the resistor values had an estimated error of about .2%.

The frequency responses of individual sections are plotted in Figures 7.4 to 7.6 together with the computed frequency responses. The clock frequency is 64 kHz, consequently the folding frequency is 16 kHz. The measured responses agree closely with the calculated responses. The frequency response of the cascade of sections is shown in Figure 7.7 for two input signal levels, together with the calculated frequency response. Close agreement is again observed. An expanded plot of the pass band frequency response is shown in Figure 7.8, demonstrating pass band ripple of about .2 dB.

Noise at the output of the filter was measured using a 30 Hz bandwidth (36 Hz "ideal" filter bandwidth) with the filter input grounded, Figure 7.9. The noise spectrum has a shape similar to the filter function, indicating that most of the

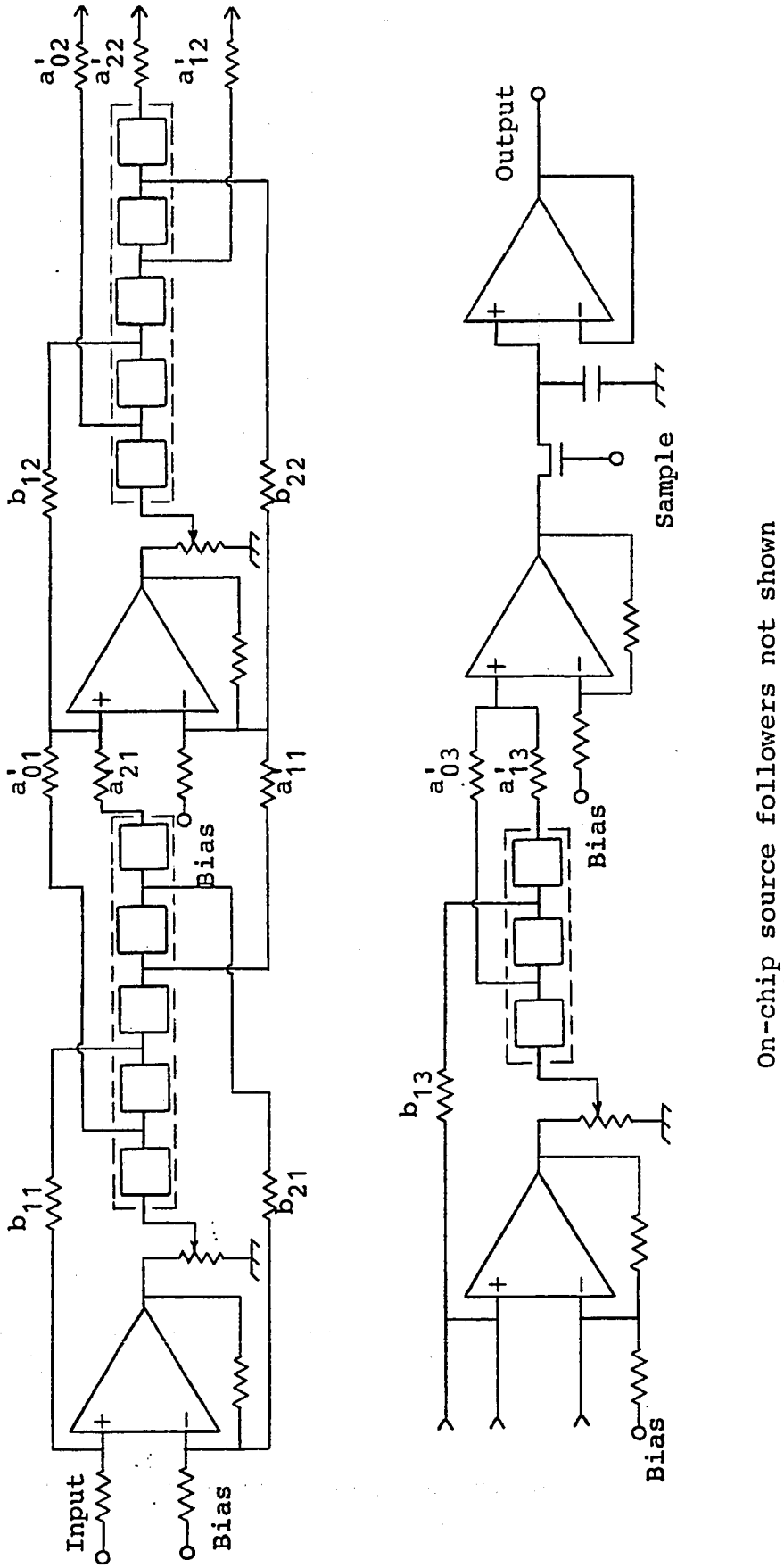

Figure 7.3 CCD Implementation of Fifth Order Lowpass Filter

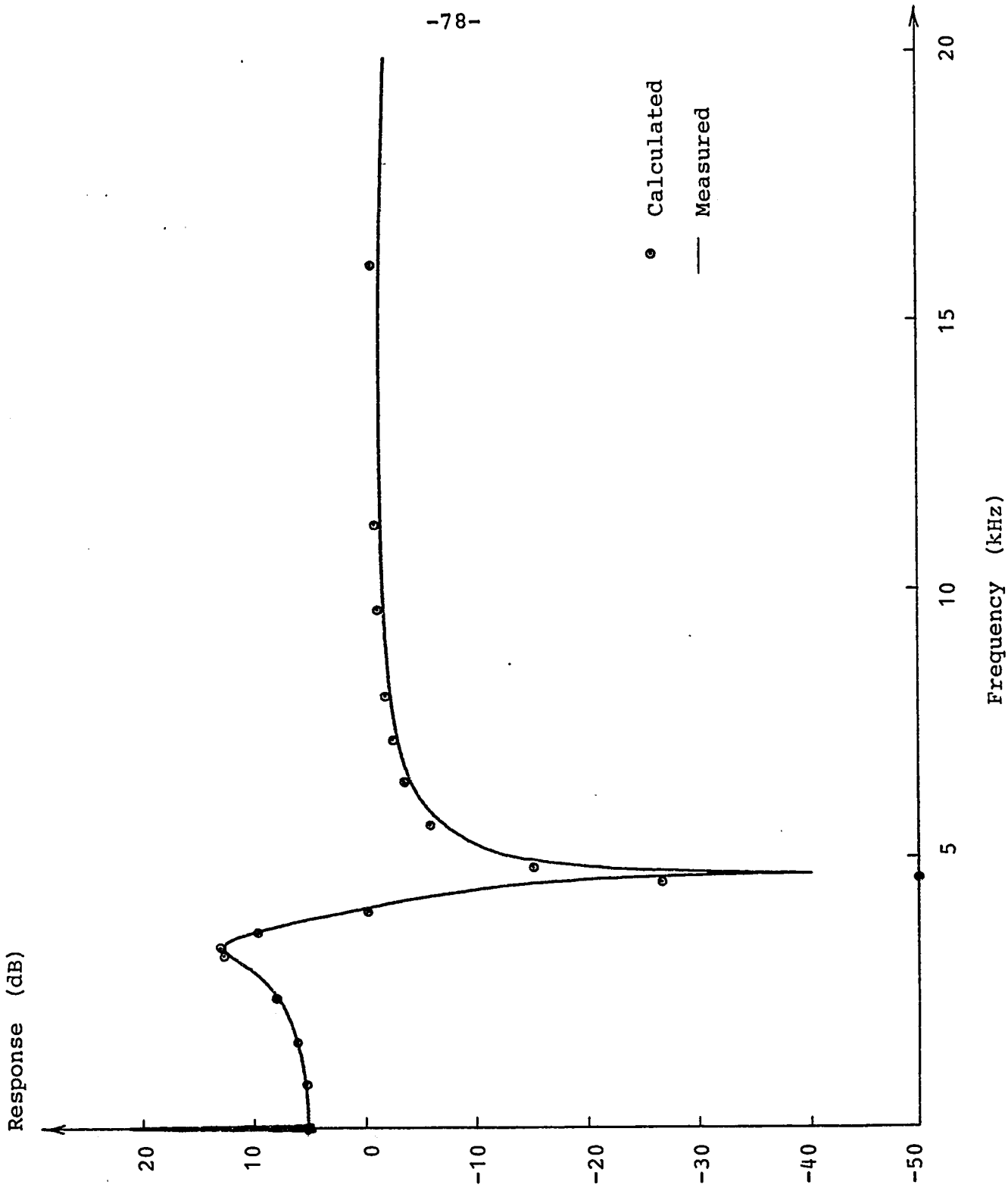

Figure 7.4 Frequency Response of Second Order Section

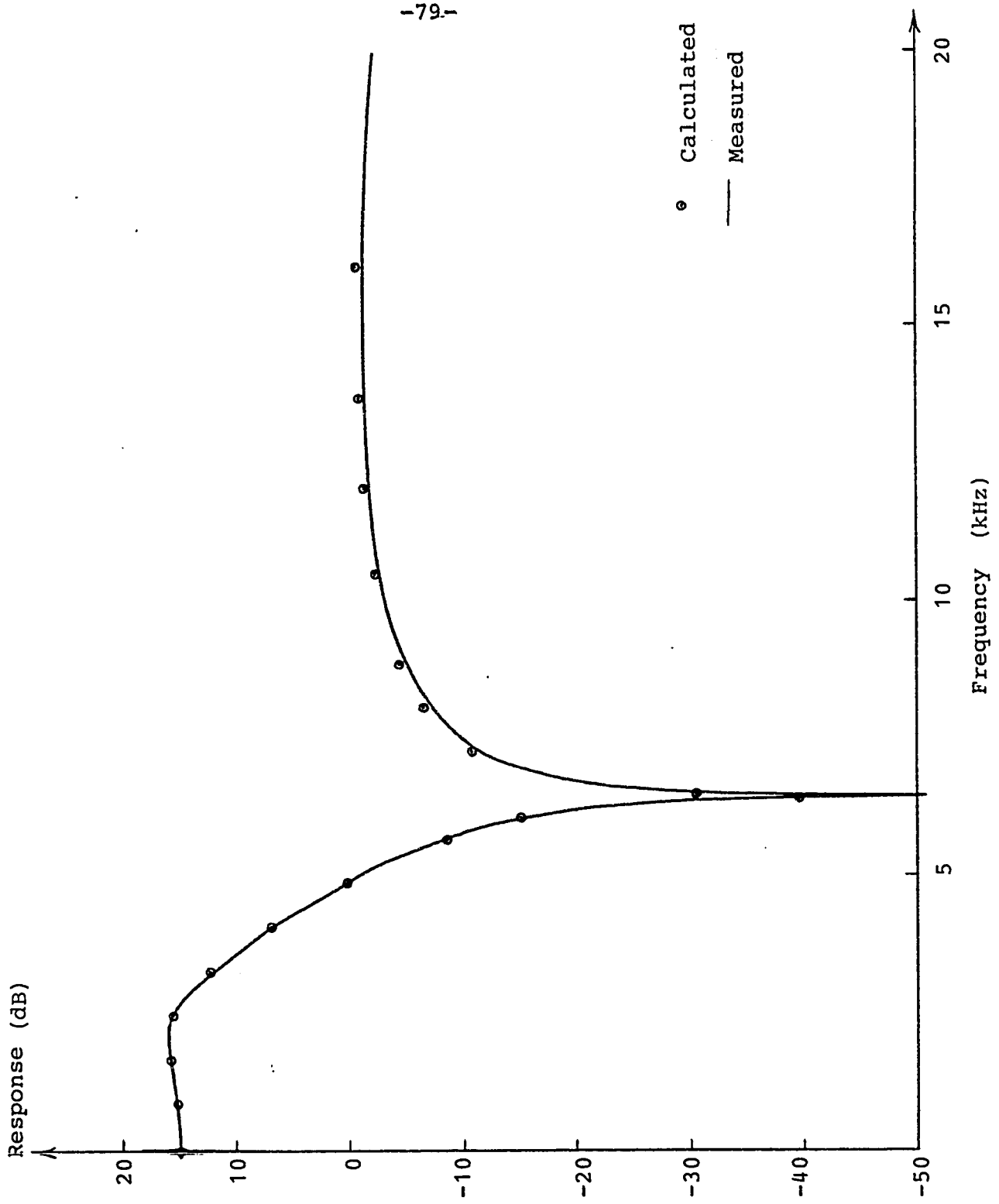

Figure 7.5 Frequency Response of Second order Section

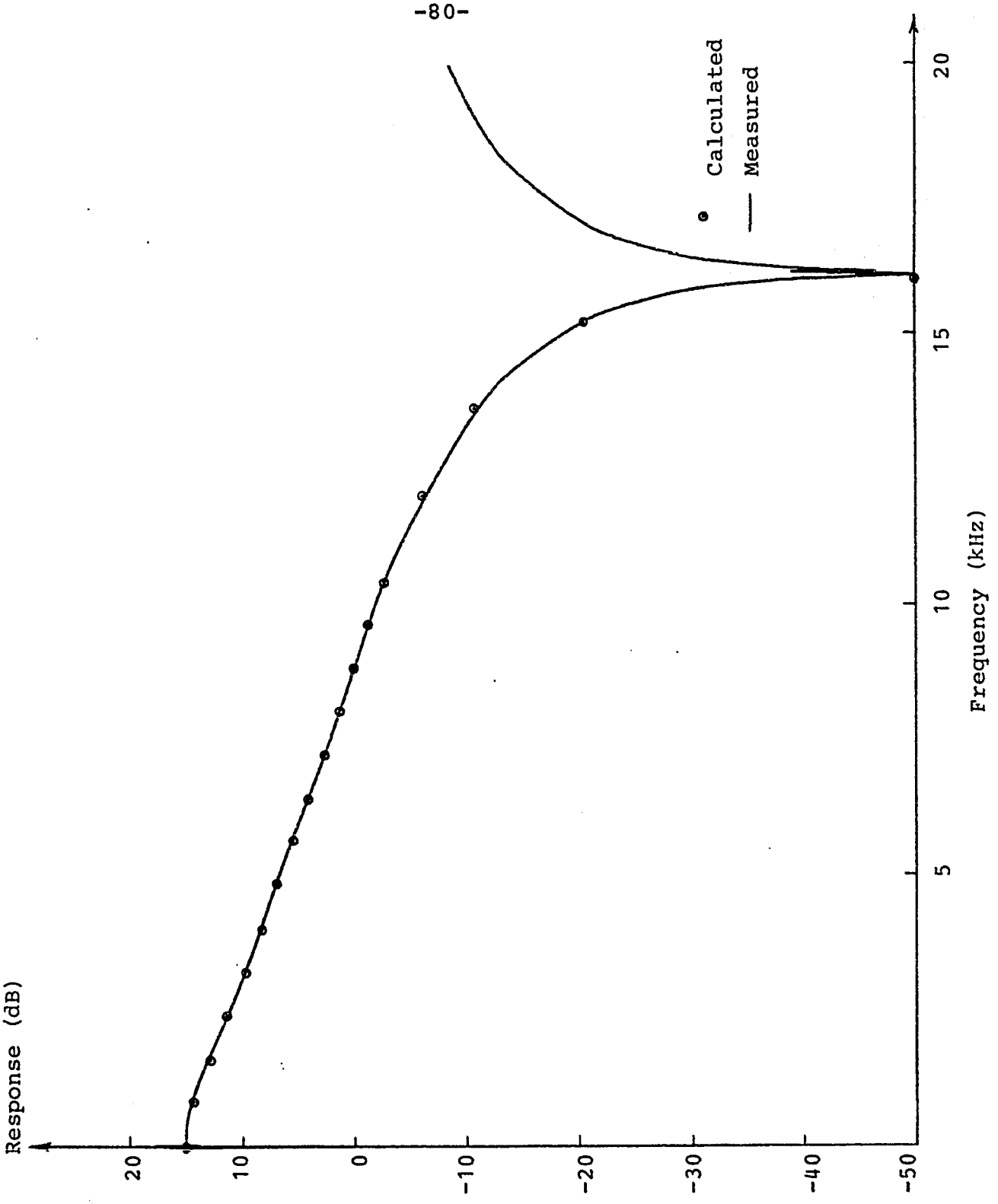

Figure 7.6 Frequency Response of First Order Section

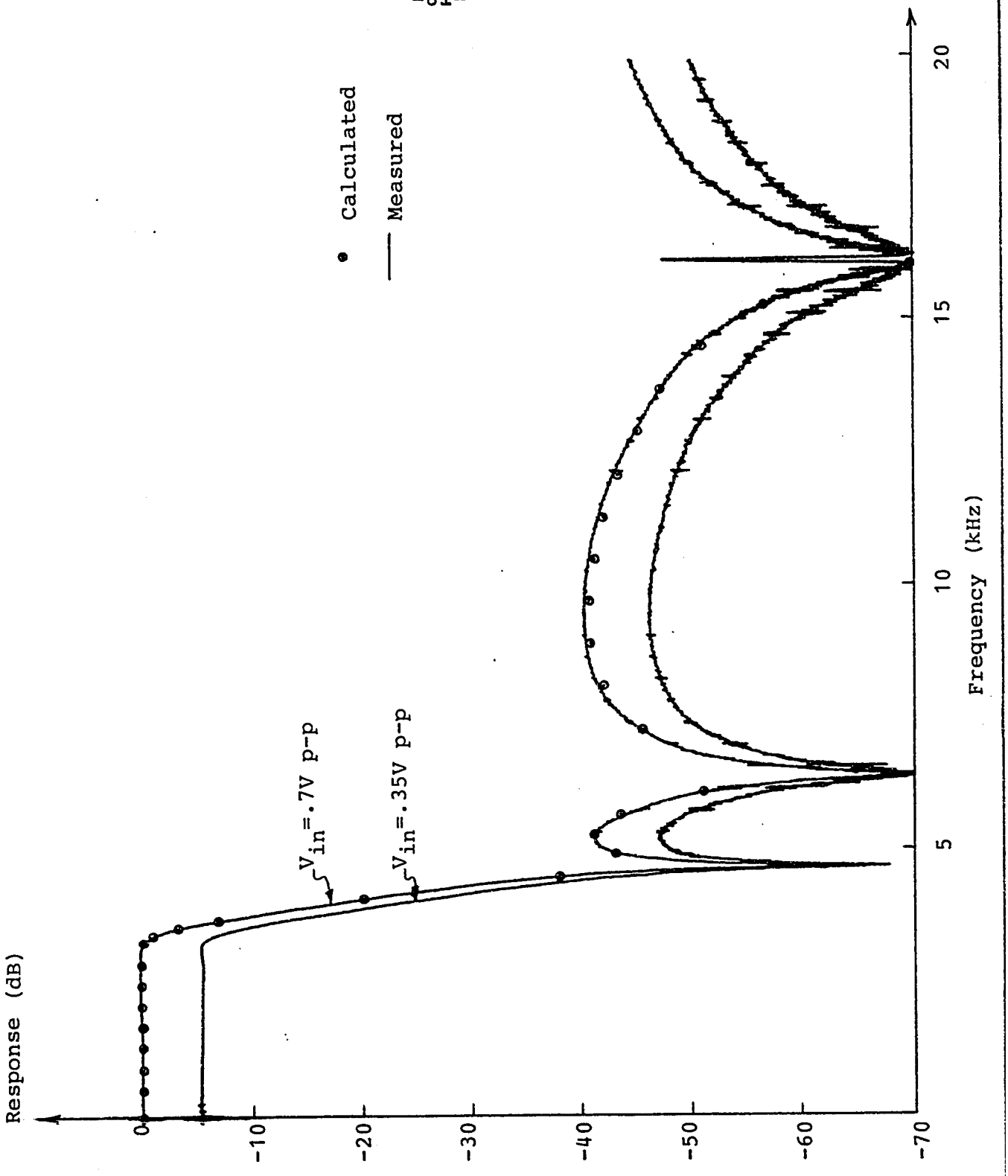

Figure 7.7 Frequency Response of Fifth Order Filter

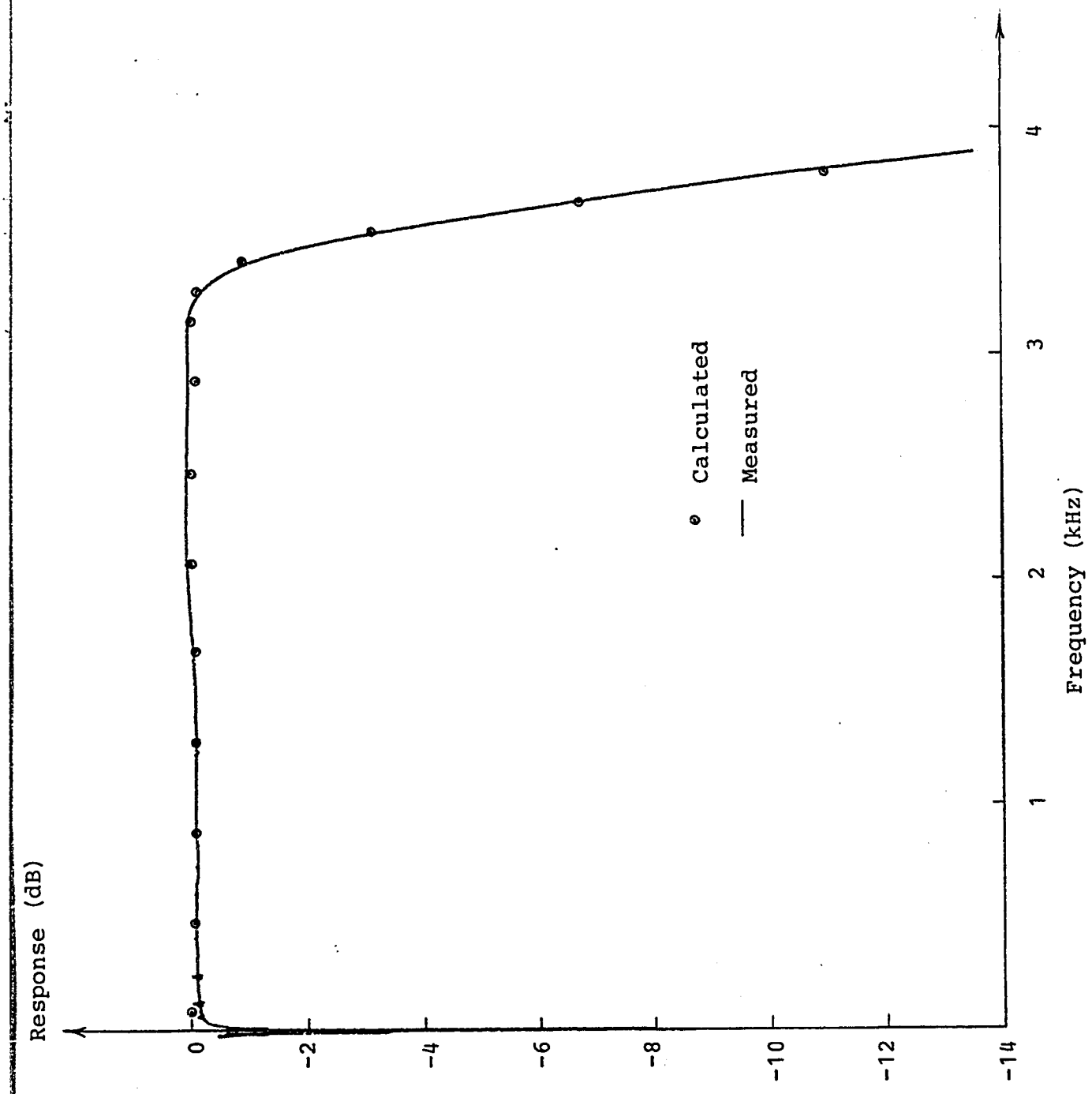

Figure 7.8 Expanded Passband Frequency Response

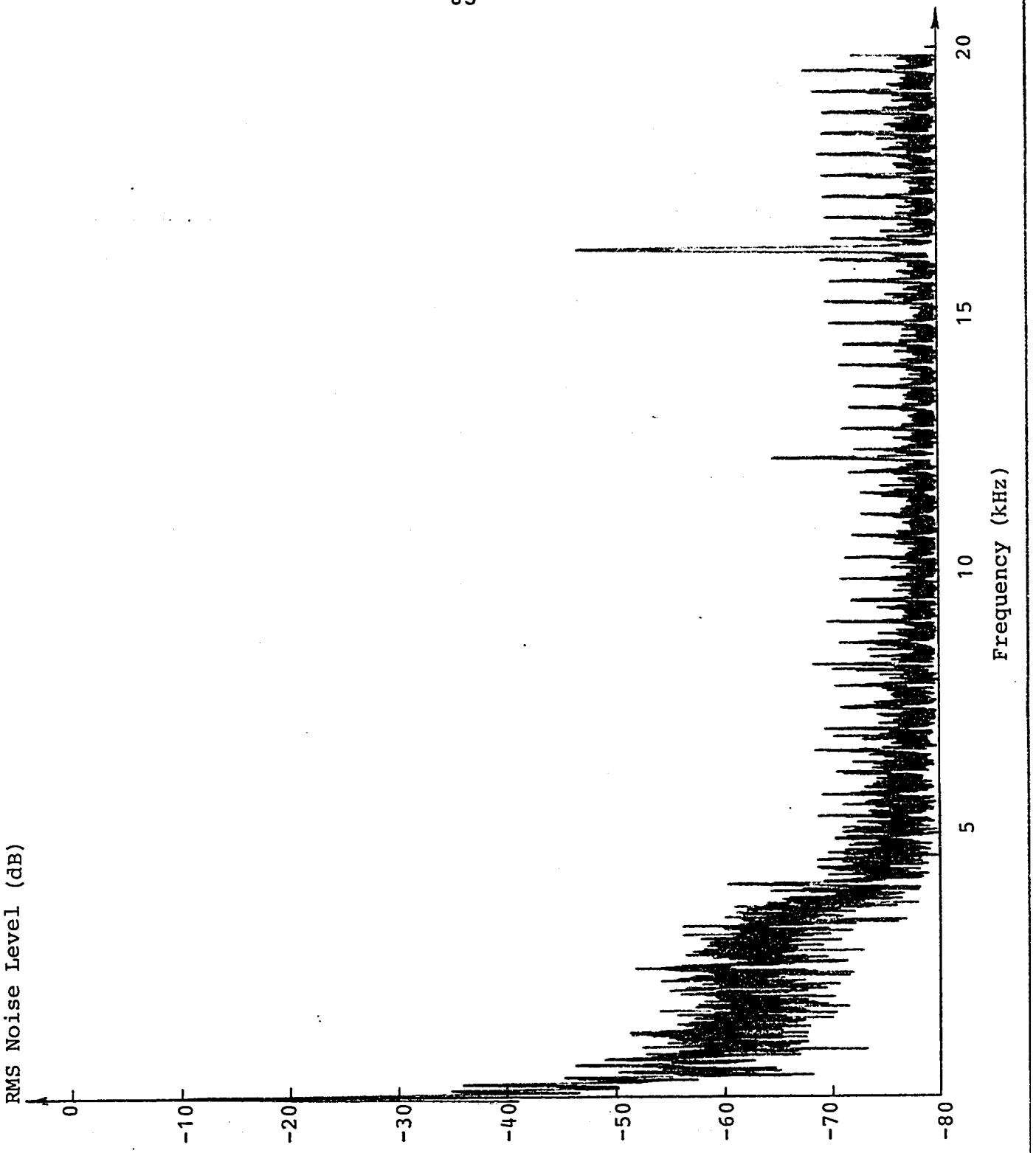

Figure 7.9 Filter Output Noise

noise originated at the input to the first second order section. Figure 7.10 is an expanded view of the noise in the filter pass band, measured in a 10 Hz bandwidth, indicating that the average noise level is 60 dB below the maximum output signal level. Power line frequency harmonics dominate the noise spectrum, however, with a peak level 36 dB below the reference level.

Harmonic distortion of the filter was measured by using a low distortion sinusoidal input signal of .7 Volts peak to peak, and observing the spectrum of the filter output. Table 7.2 gives the measured results for sinusoids of frequencies from 50 Hz to 3200 Hz.

Frequency(Hz)	Amplitude wrt Fundamental	
	2nd Harm.	3rd Harm.
50	-50 dB	-50 dB
100	-50	-52
200	-45	-44
400	-50	-50
800	-49	-50
1600	-52	-59
3200	-53	-60

Table 7.2 Filter Harmonic Distortion

The distortion of the filter at 800 Hz is similar to that measured at 700 Hz for the CCD delay line alone. At this

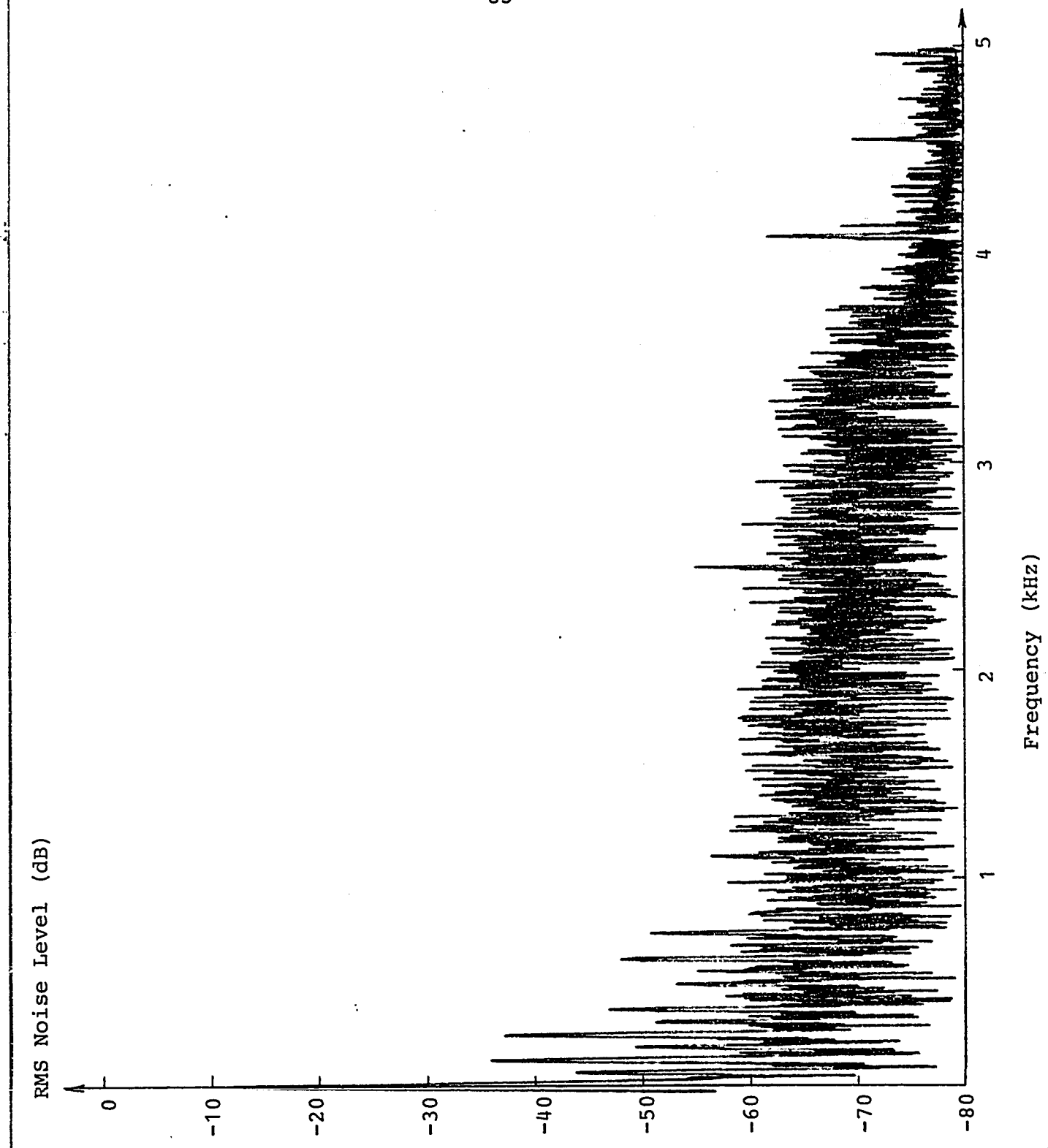

Figure 7.10 Filter Output Noise in the Passband

frequency each CCD has a different input signal magnitude; however the scaling ensures that this magnitude never exceeds .7 Volts peak to peak. Operation at smaller signal levels would reduce the amount of harmonic distortion introduced by the CCD, but would also reduce the dynamic range. The precise signal level to be used would depend on the requirements of the system of which the filter was a part.

CONCLUSIONS

8.1 Applications of CCD Recursive Filters

Three recursive CCD filters have been constructed and the results presented here. Measured results agree closely with expectations. The ability to manufacture large numbers of recursive filters with reproducible characteristics will open to the CCD a range of applications not readily accessible to transversal CCD filters.

The second order sampled data resonator, or narrow band pass filter, can be used in place of L-C resonant circuits for some applications. The filter discussed in Chapter five has the advantage that its pass band is accurately centred at one quarter of the clock frequency (except for the small effects of charge transfer efficiency). Thus the pass band frequency can be as accurately controlled as can the clock. This is a useful property for such applications as the recovery of bit timing from a random sequence of bits. An interpolation filter might be required to smooth the output signal, since at the resonant frequency a sinusoid is sampled four times per period and would give a jitter in the timing information if the zero crossings were used. The same filter can be used as a "tracking" filter, where the resonant frequency changes proportionally as the clock frequency. Such a filter could track any harmonic of a signal at the output of a network or

system, by deriving the clock rate from the fundamental of the test signal. The use of CCD recursive filters in comb filter applications has been discussed in the literature[5].

A more general second order section, where the resonant frequency can be designed to lie anywhere from zero frequency to one half the clock frequency, has application in tone detection circuits. Here it can replace the active band pass filters sometimes used at present. By incorporating the coefficient weighting and adding functions onto the same chip as the CCD, as is now done for transversal filters, the need for trimming external components will be eliminated. By suitable manipulation of the coefficients, tone filters can also become tone generators[3].

Sampled data filters of order higher than two can realize any transfer function to within a specified error, providing that N is sufficiently large. Whether or not a filter can be realized as a cascade of first and second order sections depends primarily on the coefficient accuracy which can be achieved. For coefficients based on the ratios of capacitors integrated on a silicon substrate, 0.1% accuracy has been mentioned[29]. With this accuracy, many filters with moderate transition ratios and stop band attenuation to 60 dB can be realized. The fifth order low pass filter described in Chapter seven is one such example. The frequency of operation is dependent upon limitations of the CCD and of the circuitry used for coefficient weighting and summing; however CCD clock

rates of 135 mHz have been reported[30], making the peripheral circuitry the speed limiting factor. Monte Carlo analysis of any specific design can show the practicability of realizing it or not with CCD's.

8.2 Conclusions

This work has shown that sampled data recursive filters can be realized using CCD's as the tapped delay line element, and by using operational amplifiers as coefficient weighting and summing elements. Recursive filters are capable of approximating a desired filter response with fewer delays than transversal filters, and thus promise smaller integrated circuit chip areas if the weighting and summing circuitry is sufficiently small in area. An extreme example of the benefits gained by using a recursive filter is a comparison of the sampled data resonator described in Chapter five with a 500 tap CCD transversal filter[31], which has essentially the same frequency response. The sampled data resonator has the simplest recursive filter structure, yet is useful in several applications. It has been shown that the effect of charge transfer efficiency on the frequency response characteristics of second order recursive filter sections is slight, and can be disregarded in most cases. More complex filters of order $N > 2$ should be realized by a cascade of second and first order sections in order to minimize coefficient sensitivity.

The bilinear transformation is a convenient way of using tabulated data for continuous-time filters in the design of sampled data filters. More general design methods are available, and are required for filters not having Butterworth, Chebyshev, or elliptic characteristics. The designer is free to choose the relationship of the pass band frequencies to the sampling frequency, subject to the effects of coefficient accuracy. Increasing the sampling rate with respect to the filter pass band requires greater accuracy while simplifying the aliasing problem, and vice versa. It was shown by an example that increasing the order of the filter while maintaining the same transition and stop band specifications for an elliptic filter can ease the coefficient accuracy problem.

Further work can be done in optimizing both recursive filter structures and the CCD's to realize them. The problem of output noise with respect to section ordering has been studied for digital filters[25], but should be studied for analog sampled data filters. Low sensitivity structures such as ladders[32] and wave digital filters[33] should be studied for CCD implementation. As for the CCD itself, work can be done on increasing the dynamic range by handling larger input signals at reduced distortion levels. The CCD must be optimized to have stable and predictable gain characteristics so that coefficients can be accurately realized. Split electrode coefficient weighting should be tried for recursive

filters. Finally, the possibility of using the CCD charge packets themselves as feedback signals instead of using the present voltage to charge to voltage conversions should be studied.

APPENDIX A

Quality Factor of a Z Plane Pole

An expression for the Q of a pole in the Z plane can be found by transforming the approximate expression for the Q of a pole at S_0 in the S plane:

$$Q \simeq -\frac{\omega_0}{2\sigma_0} \qquad S_0=\sigma_0+j\omega_0 \tag{A1}$$

using $Z=e^{ST}$ (standard Z transform)

$$Z_0=e^{S_0T}$$

$$r_0e^{j\theta_0}=e^{(\sigma_0+j\omega_0)T}$$

$$r_0=e^{\sigma_0T} \tag{A2}$$

$$\omega_0=\theta_0T \tag{A3}$$

substituting (A2) and (A3) in (A1):

$$Q \simeq -\frac{\theta_0T}{2T \ln r_0}$$

$$=-\frac{\theta_0}{2 \ln r_0} \qquad 0<\theta_0<\pi \tag{A4}$$

To test the accuracy of this approximation with respect to the 3 dB bandwidth formulation of Q, consider the resonator with poles at $.99217e^{\pm j\pi/2}$:

$$H(Z)=\frac{1}{1+.9844Z^{-2}}$$

$$H(e^{j\omega T}) =\left|\frac{1}{1+.9844e^{-2j\omega T}}\right|$$

$$=\frac{1}{\{(1+.9844\ \cos 2\omega T)^2+(.9844\ \sin 2\omega T)^2\}^{\frac{1}{2}}}$$

To find the frequencies at which the response is 3 dB down from the peak, set

$$\frac{|H(e^{j\omega T})|^2}{|H(e^{j\omega T})|^2_{max}} = \frac{1}{2} \; ; \quad |H(e^{j\omega T})|_{max} \text{ is at } \omega T = \pi/2$$

$$\frac{\{(1+.9844\cos 2\omega T)^2+(.9844\sin 2\omega T)^2\}^{-1}}{\{(1-.9844)^2\}^{-1}} = \frac{1}{2}$$

$$(1+.9844\cos 2\omega T)^2+(.9844\sin 2\omega T)^2 = .00048672$$

$$1+1.9688\cos 2\omega T+.96904336 = .00048672$$

$$\omega_0 T = 1.5629347,\ 1.5786580$$

Since Q can be defined as

$$Q = \frac{\text{centre frequency}}{\text{3 dB bandwidth}}$$

$$Q = \frac{\pi/2}{1.578658-1.5629347}$$

$$= 99.90$$

and from

$$Q \simeq -\frac{\theta_0}{2 \ln r_0}$$

$$Q \simeq -\frac{\pi/2}{2 \ln \sqrt{.9844}}$$

$$= 99.90$$

Thus, for large Q, (A4) gives an accurate measure of pole Q. Similarly, for a filter with $b_1=0$ and $b_2=.7304027$, Q=5.00 by calculation from (A4), and Q=4.96 by calculating the 3 dB frequencies. Thus (A4) appears to give a close approximation of Z plane pole pair Q for any value of b_2.

REFERENCES

[1] W.S. Boyle and G.E. Smith, "Charge Coupled Semiconductor Devices", Bell System Tech. J.,vol.49, pp.587-593, April 1970.

[2] D.A. Smith, C.M. Puckette, and W.J. Butler, "Active Bandpass Filtering With Bucket-Brigade Delay Lines", IEEE J. Solid-State Circuits, vol.SC-7, pp.421-425, Oct. 1972.

[3] D.A. Smith, W.J. Butler, and C.M. Puckette, "Programmable Bandpass Filter and Tone Generator Using Bucket-Brigade Delay Lines", IEEE Trans. Circuits and Systems, vol.CAS-21, pp.497-501, July 1974.

[4] J. Mattern and D.R. Lampe, "A Reprogrammable Filter Bank Using Charge-Coupled Device Discrete Analog-Signal Processing", IEEE Trans. Electron Devices, vol.ED-23, pp.156-161, Feb. 1976.

[5] T.F. Tao, V. Iamsaad, S. Holmes, B. Freund, and L. Saetre, "Sampled Analog CCD Recursive Comb Filters", Proceedings of the 1975 Int'l. Conference on the Application of Charge Coupled Devices, pp.257-266, San diego Calif., Oct. 1975.

[6] D.R. Collins, W.H. Bailey, W.M. Gonsey, and D.D. Buss, "Charge Coupled Device Analogue Matched Filters", Electron. Lett., vol.8, pp.328-329, June 29, 1972.

[7] A.A. Ibrahim, S. Ferguson, and W. Steenaart, "CCD's for Recursive Filter Applications", Device Research Conference, Salt Lake City, June 21-23, 1976.

[8] _____, op. cit.

[9] A.A. Ibrahim, L. Sellars, T. Foxall, and G. Hupe, "Evaluation of a General Purpose CCD Transversal Filter", 1976 IEEE Int'l. Solid State Circuits Conf., Digest of Technical Papers, pp.196-197.

[10] W.B. Joyce and W.J. Bertram, "Linearized Dispersion Relation and Green's Function for Discrete-Charge-Transfer Devices with Incomplete Transfer", Bell System Tech. J., vol.50, pp.1741-1759, July-Aug. 1971.

[11] A. Gersho and B. Gopinath, "Filtering with Charge Transfer Devices", IEEE Proceedings of the 1975 Int'l. Symposium on Circuits and Systems, pp.183-186.

[12] A.V. Oppenheim and R.W. Schafer, Digital Signal Processing, p.149, Prentice-Hall, 1975.

[13] _____, op. cit., p.150.

[14] J.F. Kaiser, "Some Practical Considerations in the Realization of Linear Digital Filters", Proceedings of the 3rd Annual Allerton Conf. Circuit System Theory, pp.621-633, 1965.

[15] A.V. Oppenheim and R.W. Schafer, op. cit., p.167.

[16] S.K. Mitra and R.J. Sherwood, "Estimation of Pole-Zero Displacements of a Digital Filter Due to Coefficient Quantization", IEEE Trans. Circuits and Systems, vol.CAS-21, pp.116-124, Jan. 1974.

[17] L.B. Jackson, J.F. Kaiser, and H.S. McDonald, "An Approach to the Implementation of Digital Filters", IEEE Trans. Audio Electroacoust., vol.AU-16, pp.413-421, Sept. 1968.

[18] L.R. Rabiner and B. Gold, Theory and Application of Digital Signal Processing, p.31, Prentice-Hall, 1975.

[19] B. Gold and C.M. Rader, Digital Processing of Signals, pp.70-78, McGraw-Hill, 1969.

[20] J.F. Kaiser, "Design Methods for Sampled Data Filters", Proceedings of the 1st Annual Allerton Conf. Circuit System Theory, pp.221-236, 1963.

[21] E. Avenhaus, "A Proposal to Find Suitable Canonical Structures for the Implementation of Digital Filters with Small Coefficient Wordlength", Nachrichtentech. Z., vol.25, pp.377-382, Aug. 1972.

[22] J. Szczupak and S.K. Mitra, "Digital filter Realization Using Successive Multiplier-Extraction Approach", IEEE Trans. Acoust., Speech, Signal Processing, vol.ASSP-23, pp.235-239, Apr. 1975.

[23] N.G. Kingsbury, "Second-Order Recursive Digital-Filter Element for Poles Near the Unit Circle and the Real Z Axis", Electron. Lett., vol.8, pp.155-156, March 23, 1972.

[24] C.M. Rader and B. Gold, "Effects of Parameter Quantization on the Poles of a Digital Filter", Proc. IEEE(Lett.), vol.55, pp.688-689, May 1967.

[25] L.B. Jackson, "Roundoff-Noise Analysis for Fixed-Point Digital Filters Realized in Cascade or Parallel Form",

IEEE Trans. Audio Electroacoust., vol.AU-18, pp.107-122, June 1970.

[26] W.S. Lee, "Optimization of Digital Filters for Low Roundoff Noise", Proceedings of the 1973 Int'l. Symposium on Circuit Theory, pp.381-383.

[27] A. Premoli, "The MUCROMAF Polynomials: An Approach to the Maximally Flat Approximation of RC Active Filters with Low Sensitivity", IEEE Trans. on Circuit Theory, vol.CT-20, pp.77-80, Jan. 1973.

[28] _____, "A New Class of Equal-Ripple Filtering Functions with Low Q-Factors: the MUCROER Polynomials", IEEE Trans. on Circuits and Systems, vol.CAS-21, pp.609-613, Sept. 1974.

[29] I.A. Young, D.A. Hodges, and P.R. Gray, "Analog NMOS Sampled-Data Recursive Filter", 1977 IEEE Int'l. Solid-State Circuits Conf., Digest of Technical Papers, pp.156-157.

[30] J.M. Esser, "The Peristaltic Charge-Coupled Device for High Speed Charge Transfer", 1974 IEEE Int'l. Solid-State Circuits Conf., Digest of Technical Papers, pp.28-29.

[31] R.W. Brodersen, C.R. Hewes, and D.D. Buss, "A 500-Stage CCD Transversal Filter for Spectral Analysis", IEEE Trans. Electron Devices, vol.ED-23, pp.143-152, Feb. 1976.

[32] L.T. Bruton, "Low-Sensitivity Digital Ladder Filters", IEEE Trans. Circuits and Systems, vol.CAS-22, pp.168-176, March 1975.

[33] A. Fettweis, "Digital Filter Structures Related to Classical Filter Networks", Arch. Elek. Ubertragung., vol.25, pp.79-89, Feb. 1971.